Manuscript prepared for Atmos. Chem. Phys. Discuss.
with version 2014/07/29 7.12 Copernicus papers of the LaTeX class copernicus.cls.
Date: 15 June 2015

Dust–air pollution dynamics over the Eastern Mediterranean

M. Abdelkader[1], S. Metzger[1,2], R. E. Mamouri[3], M. Astitha[4], L. Barrie[5], Z. Levin[1,6], and J. Lelieveld[1,2]

[1]Energy, Environment and Water Research Center, The Cyprus Institute, Nicosia, 2121, Cyprus
[2]Air Chemistry Department, Max Planck Institute for Chemistry, Mainz, 55128, Germany
[3]Department of Civil Engineering and Geomatics, Cyprus University of Technology, Limassol, 3036, Cyprus
[4]Department of Civil Engineering, University of Conneticut, Storrs-Mansfield, 06269, USA
[5]Department of Geological Sciences, Stockholm University, Stockholm, SE-106 91, Sweden
[6]Tel Aviv University, Tel Aviv, 39040, Israel

Correspondence to: M. Abdelkader (m.abdelkader@cyi.ac.cy), S. Metzger (s.metzger@cyi.ac.cy)

Abstract

Interactions of desert dust and air pollution over the Eastern Mediterranean (EM) have been studied, focusing on two distinct dust transport events on 22 and 28 September 2011. The atmospheric chemistry–climate model EMAC has been used at about 50 km grid spacing, applying an online dust emission scheme and calcium as a proxy for dust reactivity. EMAC includes a detailed tropospheric chemistry mechanism, aerosol microphysics and thermodynamics schemes to describe dust "aging". The model is evaluated using ground-based observations for aerosol concentrations and aerosol optical depth as well as satellite observations. Simulation results and back trajectory analysis show that the development of synoptic disturbances over the EM can enhance dust transport from the Sahara and Arabian deserts in frontal systems that also carry air pollution to the EM. The frontal systems are associated with precipitation that control the dust removal. Our results show the importance of chemical aging ~~and deposition of the dustduring transport~~of dust, which increases particles size, dust deposition and scavenging efficiency during transport, overall reducing the life-time relative to non-aged dust particles. The relatively long travel periods of Saharan dust result in more sustained aging compared to Arabian dust. Sensitivity simulations indicate three times more ~~rapid~~ dust deposition of aged relative to pristine dust, which significantly decreases the dust lifetime and loading.

1 Introduction

1.1 Importance of atmospheric dust

The atmospheric dust cycle, a fundamental component of the Earth System, can strongly influence air quality and climate. Atmospheric dust causes a radiative forcing of climate by direct and indirect effects. Dust particles scatter solar shortwave radiation back to space, which can enhance the Earth's albedo. Indirect effects result from dust particles acting as cloud condensation nuclei (CCN), which can affect the droplet number concentration and reflectivity of clouds, and either enhance (Yin et al., 2002) or suppress (Rosenfeld et al., 2001)

precipitation formation depending on their mineralogy and solubility. Furthermore, pristine dust particles are the best natural ice nuclei (IN), especically over the Easter Mediterranean (EM) region (Ardon-Dryer and Levin, 2014). Moreover, dust particles provide a surface for heterogeneous chemical reactions, which affects dust–climate interactions (Dentener et al., 1996; Bauer et al., 2004; Mogili et al., 2006; Bauer et al., 2007; Astitha et al., 2010; Crowley et al., 2010, among others). Dust influences a wide range of atmospheric physical, chemical and biogeochemical processes, including the marine and terrestrial biosphere through the transport of nutrients like iron (Mahowald et al., 2009) and phosphorus (Nenes et al., 2011).

The impact of atmospheric dust on the Earth's climate is controlled by the balance between the emissions and the removal of the dust from the atmosphere, which is altered by chemical and physical processes that occur during transport. This "aging" process poses one of the challenges in quantifying the direct and indirect radiative forcing of mineral dust. It is one of the central uncertainties in modeling the dust cycle in climate, atmospheric chemistry and Earth system models (Stocker et al., 2014) especially in view of dust removal by wet deposition (Schulz et al., 2012). Therefore, an accurate modeling of mineral dust emissions, transport, and chemistry is required to enhance our quantitative understanding of the global dust abundance, dust storm episodes and their impacts on climate, air quality and biogeochemical cycles.

1.2 Dust transport

The transport of Saharan dust in addition to that from the Middle East deserts are the main sources of atmospheric dust in the EM region (Pey et al., 2013), being a regular atmospheric phenomenon in this region (Ganor et al., 2010). Typically, the majority of dust outbreaks are related to steep surface pressure gradients between northern Africa and the Mediterranean (Dayan et al., 2008). Saharan dust is generally mobilized in Libya, Egypt and the Bodele Depression (Pey et al., 2013) during the local dry season from October to April (Goudie and Middleton, 2006) and then transported over the EM by Sharav cyclones (Ganor and Mamane, 1982; Moulin et al., 1998; Goudie and Middleton, 2006; Ganor et al., 2010) or Khamasin events (Ganor and Mamane, 1982). These cyclones are gener-

ated along the polar front and subtropical jet streams (Kallos et al., 2006) as a result of differential heating between relatively colder oceanic waters to the north and warmer land masses to the south (Goudie and Middleton, 2006). These synoptic conditions are usually associated with a cold front and are often accompanied by rain over the EM (Alpert and Ganor, 1993). In addition, the EM is affected by dust transport from the Negev desert, controlled by a range of synoptic systems, e.g., Cyprus Lows, Red Sea troughs, Persian troughs, anticyclones over the Levant and to the east of the region. The majority, i.e., about two thirds of the yearly dust events are caused by Cyprus lows (Dayan et al., 2008). Since Cyprus lows are often associated with precipitation, the residence time of dust particles in the atmosphere can be relatively short~~(approximately one day). Dayan et al. (1991, 2008) .~~ In case of a barometric trough penetrating from the Red Sea into the EM, it can be as short as one day (Dayan et al., 1991) . Dayan et al. (2008) studied events where dust is transported from the Sahara, indicating that the average residence time is about four days before the dust is removed by rain. The combination of dust transport from the Sahara and Middle East deserts result in numerous and very intense dust episodes over the EM and Cyprus (Pey et al., 2013). In general, the transport of Saharan dust usually extends into relatively deep atmospheric layers and is characterized by a regional extension over the Mediterranean Basin. Typically, dust is transported over the EM at an elevation between 1.5 up to 6.5 km above sea level and commonly at about 2.5 km (Levin et al., 2005; Papayannis et al., 2005; Ganor et al., 2010; Mamouri et al., 2013). Since Saharan dust events last longer and have higher mass loadings compared to the Negev and Middle East desert dust events, they may have stronger impacts on the EM region (Dayan et al., 1991), however, there are large uncertainties. Especially the interaction ~~between dust and anthropogenic~~ of atmospheric dust particles with air pollution from eastern and western Europe ~~(Levin et al., 2005) in addition to intercontinental air pollution transports from North~~ and long-range transport from north America and Asia ~~(Lelieveld et al., 2002) deserves attention, being~~ (Lelieveld et al., 2002; Levin et al., 2005, among others) remains to be scrutinized – the focus of this study.

1.3 Dust–air pollution interactions

During transport dust undergoes chemical aging as a result of the condensation of low or semi-volatile compounds on the particle surface. The chemical aging of the dust particles can affect water uptake, which in turn controls the gas-liquid-solid partitioning of various gaseous compounds, including sulfuric, nitric and hydrochloric acid. Previous studies (Levin et al., 1996) have focused on the dust coating by sulfate and the resulting effect on rain formation in the EM. More recent modeling studies addressed the relative importance of mineral cations and organics on the gas-aerosol partitioning of reactive nitrogen compounds, since cations such as calcium largely determine the neutralization level of sulfate, nitrate, chloride and organic compounds (Trebs et al., 2005; Metzger et al., 2006). In addition, various other heterogeneous reactions occur on the dry surface of dust particles that may depend on their mineralogy and alkalinity. Soluble compounds eventually alter the dust chemical composition, shape and size distribution and the atmospheric lifetime. Chemical aging of dust particles may further control the activation of CCN, reduce the IN efficiency (Reitz et al., 2011), or affect the scavenging efficiency (Manktelow et al., 2010). Typically, the atmospheric lifetime of dust particles depends on (1) dry removal, which mainly depends on the ambient (wet) particle size and (2) on wet deposition. The latter includes in- and below cloud scavenging, and depends on the chemical composition of the dust surface, which can include a large fraction of water in case dust particles are coated by hydrochloric or nitric acids and/or are exposed to high relative humidity. The fraction of coated dust surface, however, critically depends on the aging mechanism. Changes in composition, size and shape of the dust particles due to the various aging processes affect the associated radiative forcing. Scattering and adsorption of sunlight is important for the influence of dust on the Earth's climate. However, to what extent chemical aging of mineral dust is important for the climate feedback mechanisms is largely unknown (Koop and Mahowald, 2013).

1.4 Dust–air pollution modeling – this study

This work presents a modelling case study based on the atmospheric chemistry – climate model EMAC. The model setup includes a detailed treatment of dust aging, which is based on the condensation of different soluble compounds and the associated water uptake of various atmospheric particles and a chemical speciation of mineral dust and sea salt compounds, which are calculated online. Dry and wet dust removal are based on the ambient particle radius and pH dependent scavenging processes. The EMAC set-up is described in Sect. 2 and evaluated in Sect. 3.1 based on various long-term observations. In Sect. 3.2 we focus on the dynamics of two distinct events where dust-air pollution interactions over the EM play a role. Sect. 3.3 analyzes the dust outflow dynamics of the case studies, while Sects. 3.4 and 3.5 investigate the effects of dust aging. We conclude with Sect. 4.

2 Model description

The ECHAM5/MESSy2 atmospheric chemistry (EMAC) model is used to study dust-air pollution dynamics over the EM. EMAC is a numerical chemistry and climate simulation system that is based on sub-models that describe tropospheric and middle atmosphere processes and their interactions with oceans, land and human influences (Joeckel et al., 2010). This Modular Earth Submodel System (MESSy) links multi-institutional computer codes. The core atmospheric model is the 5th generation European Centre Hamburg Atmospheric general circulation Model (ECHAM5, Roeckner et al. (2006)). For the present study we applied EMAC (ECHAM5 version 5.3.02, MESSy version 2.41) with the submodels AEROPT, CLOUD, CONVECT, CVTRANS, DDEP, GMXE, JVAL, LNOX, MECCA, OFFEMIS, ONEMIS, RAD4ALL, SCAV, SEDI, TNUDGE, TROPOP (http://www.messy-interface.org/). For the global anthropogenic emissions we follow Pozzer et al. (2012) and de Meij et al. (2012) and use the EDGARv4 inventory, which has been prepared in the framework of the CIRCE project with a focus on the Mediterranean region (http://www.circeproject.eu). The emission inventory includes greenhouse gases, NO_x, CO, NMVOCs, NH_3, SO_2, black carbon (BC)

and organic carbon (OC) from fossil fuel and biofuel use. The emissions are geographically distributed according to the EDGAR4 2009 database which has a monthly resolution. The monthly large-scale biomass burning emissions of OC, BC and SO_2, are based on GFED version 3 (Global Fire Emissions Database) (van der Werf et al., 2010).

The aerosol set up has been described in detail by Pringle et al. (2010); Tost et al. (2010); de Meij et al. (2012); Pozzer et al. (2012). The set up is based on the aerosol microphysics sub-model GMXe, described in Pringle et al. (2010), which is coupled to the gas–aerosol partitioning scheme ISORROPIA-II (Fountoukis and Nenes, 2007). ~~GMXe describes the aerosol size distribution in seven log-normal modes, i.e., four soluble~~ Our model version distinguishes aerosol particles in 7 modes, 4 Soluble (nucleation, aitken, accumulation~~and~~ , coarse) and three ~~insoluble~~ INSoluble modes (aitken, accumulation~~and coarse) . Mineral dust emissions are calculated online each model time step and emitted in two insoluble modes (accumulation andcoarse) following Astitha et al. (2012) . Insoluble dust particles are~~ , coarse) with the complexity of the aerosol thermodynamics as investigated in Metzger et al. (2006) , by considering case F4 since ISORROPIA-II used here does not include organic salt compounds in the gas/aerosol partitioning and aerosol neutralization framework. Within EMAC, the dust particles are emitted online following Astitha et al. (2012) (e.g., governed by model dynamics, precipitation and soil moisture) in either the INSoluble accumulation and/or coarse mode and only upon aging and transport they can be transferred to the ~~soluble modesupon chemical aging within GMXe~~respective Soluble accumulation and/or coarse modes. The aging depends on the available condensable compounds calculated within the chemistry scheme (Sander et al., 2005)~~and partition into the aerosol phase by the aerosol thermodynamic scheme (Fountoukis and Nenes, 2007)~~ . In addition, via coagulation and hygroscopic growth the size-distribution can change and small particles are transferred to larger sizes, i.e., for dust from accumulation to coarse, whereby hygroscopic growth of bulk dust and dust salt compounds is only allowed in the soluble modes.

For proper representation of chemical aging, we use a comprehensive chemistry scheme that allows the production of different aerosol precursor gases, i.e., the major inorganic

acids (H_2SO_4, HNO_3, HCl) which are all subsequently considered for the chemical aging of dust and other primary aerosol particles (i.e., BC and OC). The condensation of the acids yields anions, i.e., sulfates (SO_4^{2-}), nitrates (NO_3^-), and chlorides (Cl^-), respectively, while the additional condensation of ammonia (NH_3) yields a semi-volatile cation (NH_4^+) and can neutralize the anions leading to hygroscopic salt compounds that coat (age) the dust particles. This transformation changes the solubility of the originally insoluble pristine particles, which in turn alters the aerosol size distribution. The latter is a key parameter and important for aerosol-radiation feedbacks and aerosol in-cloud processing (nucleation scavenging) and below cloud processing (impaction scavenging). The scavenging processes applied in our study are based on Tost et al. (2006) and include a detailed scavenging chemistry that fully couples the aerosol and gas phase chemistry with liquid cloud water and ice crystals.

To additionally account for the major mineral cations, we have extended our EMAC version to include a simple chemical speciation of the natural aerosol emission fluxes. We consider the calcium cation (Ca^{2+}) as a chemically reactive tracer on the dust, being emitted in the insoluble accumulation and insoluble coarse modes as a fraction of the dust emission flux (25 and 5 % for the accumulation and coarse mode, respectively). ~~Additionally, we consider potassium () as a tracer of biomass burning emissions, being emitted here only in the insoluble aitken mode.~~ We apply chemical speciation for the bulk sea salt emission flux, i.e., we consider the cations sodium (Na^+), potassium (K^+), magnesium (Mg^{2+}), calcium (Ca^{2+}) and the anions chorine (Cl^-) and sulfate (SO_4^{2-}) ~~.as tracers for the online calculated~~ sea salt emissions. Additionally, K^+ is used for biomass burning emissions being emitted here only in the insoluble aitken mode. This chemical speciation has been determined such that the model concentrations best match the available EMEP and CASTNET measurement data for the period 2000–2013 (to be published separately). For the importance of mineral cations in gas–aerosol partitioning modelling studies with a focus on the EM we refer to Metzger et al. (2006).

The dust particles can be present in our set-up in four modes, each represented by various calcium compounds that chemically characterize the bulk dust emissions depending on the level of aging. We account for the water uptake of various major mineral salt

compounds, i.e., $CaSO_4$, $Ca(NO_3)_2$, $CaCl_2$, $MgSO_4$, $Mg(NO_3)_2$, $MgCl_2$, Na_2SO_4, $NaNO_3$, NaCl, K_2SO_4, KNO_3, KCl, but we have limited the dust neutralization reactions in this work to calcium to be able to separate the dust associated water uptake and associated aging from sea salt effects. Since our set-up is flexible, the level of aerosol neutralization complexity can/will be changed for other application tasks.

Within GMXe, the aging of dust aerosols depends on the total particle surface area and on the concentrations of the aerosol precursor gases (Pringle et al., 2010) . The uptake of gases is kinetically limited considering random motion and diffusion processes that govern the condensation. The rate constant for the condensation on dust particles is given by Eq. 1

$$D_{flux} = \frac{4\pi D_f^2 r_w}{\frac{4D_f}{\nu r_w a_i} + \frac{r_w}{r_w + z_{f1}}} \quad (1)$$

where r_w is the ambient (wet) radius, D_f the temperature dependent diffusion coefficient defined by $D_f = 0.073\, P \left(\frac{T}{T_{ref}}\right)^{\frac{3}{2}}$, P the pressure, T the temperature and T_{ref} the reference temperature (298.15 K), ν denotes the particle mean velocity, defined by $\sqrt{\frac{8R_gT}{\pi M_g}}$, with R the gas constant (8.31 $J\,mol^{-1}\,K^{-1}$), M_g the molar mass, z_{f1} the mean free path length of the kinetic regime, and a_i the accommodation coefficient (Fuchs and Davies, 1989; Seinfeld and Pandis, 2006) . In the current setup we use the accommodation coefficients 0.1, 0.01, 0.01 for sulfuric, hydrochloric and nitric acid, respectively. These values have been empirically determined by a comprehensive modeling analysis, which will be presented separately. The uptake of acids is calculated for each particles size, i.e., for dust for the insoluble accumulation and coarse mode. For the current modeling study though, this set-up represents the dust air-pollution dynamics over the Eastern Mediterranean well.

To test the relevance of higher resolution simulations for an optimal dust representation in climate models, as emphasized by Gleser et al. (2012), we apply in this study EMAC at the

spherical truncations T106 and T255, which correspond to quadratic Gaussian grids in latitude and longitude of approximately $1^\circ \times 1^\circ$ and $0.5^\circ \times 0.5^\circ$ (approximately 110 and 50 km), respectively, with 31 vertical hybrid pressure levels up to 10 hPa. Our model simulation period covers the years 2010 and 2011, in which we focus on two moderate dust events in late September 2011, since at the end of the summer dry season the air pollution build-up reaches a maximum in the EM. The EMAC meteorology is nudged towards ERA-Interim reanalysis data by a newtonian relaxation data assimilation method to best represent the actual meteorological conditions (Roeckner et al., 2006). The AEROPT submodel is used to calculated aerosol optical depth (AOD), based on internal mixture assumption of different aerosols, using the aerosol information from the GMXe aerosol submodel. The modeled AOD at 550nm wavelength is compared to the measured AOD from the sun photometer instruments in the AErosol RObotic NETwork (AERONET) (http://aeronet.gsfc.nasa.gov) over the entire period of the simulation. AERONET (Holben et al., 1998) provides the AOD at different wavelengths (340, 380, 440, 500, 670, 870, 940, 1020 nm). Only Level 2.0 direct sun algorithm wavelengths (cloud free conditions) is used in this study to calculate AOD at 550 nm for direct comparison with the modeled AOD following de Meij and Lelieveld (2011) (Eqs. 1 and 2). In order to increase the number of the calculated 550 nm data points, we calculate the 550 nm AOD from different wavelengths starting from closest to 550 nm depending on the availability of the AERONET data. For instance, the AOD at 500 and 670 nm wavelengths are used to interpolate to 550 nm. We repeat this procedure for all available wavelengths at each station. For comparison of the time history, the calculated 550 nm AOD from AERONET is averaged over the model output frequency (5 h) for a time consistent comparison. Additionally, skill scores are used to describe the model performance on a single station scale following Taylor (2001) – Eq. 4. The skill score accounts for the model bias and variance and helps evaluating the model performance.

3 Dust–air pollution interaction

Two distinct dust transport events are the basis of our study of dust-air pollution interactions over the EM. The selected cases represent moderate dust outflow accompanied by air pollution transport from Europe in addition to the local sources of air pollution in the EM. The prevailing synoptic conditions of the EM, schematically shown in Fig. 1, are characterized by a Cyprus low and main transport paths of dust and air pollution to the EM. During both dust events polluted air masses from central and southern Europe are carried into the low pressure system. Dust event outflow-1 originates from the Sahara and is transported over the EM as a result of the high pressure system over the Sahara and the low pressure system over Cyprus. The latter also enhances the transport of air pollution from Europe. Both air pollution and dust are transported over the EM in a frontal system, which is typically associated with precipitation events (Alpert and Ganor, 1993) – shown in the low pressure area (Fig. 1). During the second event strong winds and a high pressure system over the Arabian Peninsula resulted in dust transport from the Negev, Sinai and Arabian deserts to the EM (outflow-2). Several measurement stations, used in the study to evaluate the model results, are included in the map (Fig. 1).

3.1 Long-term model evaluation

Understanding the interaction between dust and air pollution over the EM requires a realistic representation of aerosols and their precursor gases (e.g., strong acids) in the EMAC model. To evaluate the model set-up of our global simulations, we first consider a two year simulation at reduced resolution (T106L31, about 110 km grid spacing).

Figure 2 shows the calculated mean aerosol mass fraction of the fine and the coarse mode for the EMEP station CUT-TEPAK in Cyprus. Sulfate (46 %) and ammonium (17 %) dominate the fine mode, while (bulk) sea salt (44 %) and dust (37 %) dominate the coarse mode. Although these model results are shown for Cyprus, they also resemble the aerosol mass fractions obtained during the MINOS campaign (Metzger et al., 2006), which was carried out over Crete in the summer 2001 (Lelieveld et al., 2002).

Figure 3 shows monthly average time series of modeled and observed aerosol properties: sulfate, calcium, total (dry) particulate matter (PM2.5) at the EMEP station Ayia Marina and the AOD at the AERONET station CUT-TEPAK. The linear distance between the two stations is about 40 km and both are located in one model grid box at T106 resolution. Generally, the EMAC results compare well with these observations. The model captures the seasonal variability of sulfate, although the highest concentration during summer and early autumn are somewhat too low. EMAC seems to underestimate the high production yields of sulfates during summer, which mainly results from the oxidation of the precursor gas SO_2, enhanced by the prevailing subsidence of air over the EM region. For calcium, the model captures the concentration peaks, which correspond to the dust outflow into the Mediterranean from both the Saharan and Middle East deserts during the spring season. Capturing the peak concentrations of calcium shows the capability of EMAC to simulate the dust outflow throughout the year. Furthermore, simulated total PM also shows good agreement with the observed concentrations and the seasonality. However, the model captures the seasonality of PM in the year 2011 better than in 2010, partly related to the model spin up time in this year. The PM is the total (dry) mass of all aerosols considered in this set up, and is explicitly calculated from aerosol microphysics and thermodynamics as described in Pringle et al. (2010). These results are supported by the AOD comparison, corroborating that EMAC captures the observations. Considering that the PM and AOD are two independent observations, in addition to the independent species sulfate and calcium, these results confirm that this model configuration is capable of simulating the major aspects of atmospheric composition, needed to study the interaction between dust and air pollution.

3.2 EMAC case study

An episode of low visibility occurred over Cyprus in late September, 2011 as a result of increased atmospheric dust concentrations. Two dust events were reported, the first event started on 20 September and originated in the Sahara while the dust was removed mainly by precipitation over Cyprus. The second event started on 26 September from the Middle East deserts and the dust was transported over the EM and removed mainly by dry deposi-

tion. The two episodes are investigated using the high resolution model version (T225L31, about 50 km grid spacing), using the same EMAC set-up mentioned above.

3.2.1 Aerosol Optical Depth (AOD)

Figure 4 shows the AOD time series over six AERONET stations in the eastern Mediterranean and Middle East region in September 2011, which capture the selected dust episode. The periods of the two dust outflow events are delineated (orange box in ATHENS-NOA, CUT-TEPAK and Tuz_Golu_2 stations). In general, the model reproduces the variability and magnitude of the AOD observations in the EM region. During the first dust event (17–22 September, 2011), the modeled and observed AOD are about 0.4 in the dust outflow region, which extends to Athens-NOA and Tuz_Golu_2. At CUT-TEPAK the observed AOD of 0.6 is higher and slightly above the modeled AOD. At Sede Boker and Eilat, being closer to the dust source area for the dust outflow-2 event, the model results are in good agreement with the observations. Eilat, however, is strongly impacted by local sources during the 2nd dust event and the observed AOD up to 1.0 is underestimated by the model, despite the relatively high model resolution (50 km grid box). Eilat is located at the coast in a valley between mountain ranges in Egypt, Jordan and Israel. The model may not capture the magnitude of the dust AOD but does reproduce the variability at this station, despite the complexity of the terrain at the Eilat site for which our 50 km model resolution might be too coarse. Possibly some of the high AOD is explained by local course mode dust particles that rapidly sediment and contribute little to long-distance transport. Figure 5 shows the AOD (monthly mean) over the EM region during September 2011, including AERONET observations and corresponding skill scores. The comparison indicates good agreement with skill scores above 0.5, while the model tends to slightly underestimate the AOD. Both model and observations show for this month similar AOD patterns, which increase eastwards. Highest skill scores are, however, achieved at ATHENS-NOA, Greece (0.8) and Tuz_Golu_2 (0.9), Turkey. In the Negev and Arabian deserts AODs are highest due to strong emissions at this time, which is captured well by the model. In addition, where the primary dust is the dominant aerosol (in EMAC), the model AOD compares better with observations than at

locations that are affected by aged dust, e.g., over Cyprus (CUT-TEPAK). Generally, stations with aged dust particles show reduced agreement with observation. In addition to the aerosol dust loading (number and mass concentrations), the relative humidity and aerosol composition (e.g., as a function of air pollution) become important, as both determine the aerosol water uptake, which in turn affects the AOD.

3.3 Dust outflow characteristics

The true color image from the Moderate Resolution Imaging Spectro-radiometer (MODIS)-Aqua instrument, Fig. 6, shows both dust events over the EM. Figure 7 shows the daily average, vertically integrated dust load over the EM region for both dust events and HYSPLIT (http://ready.arl.noaa.gov/) backward trajectories, which show the pathways of the air masses that reached the CUT-TEPAK station on the 22 and 28 September 2011. The HYSPLIT trajectories are driven by NCEP (National Center for Environmental Prediction) reanalysis data that appear to be consistent with our model calculations. The streamlines and the velocity vectors refer to an elevation of about 2.5 km (700 hPa) and show the maximum dust concentration during atmospheric transport. In the dust outflow-1 event (Fig. 7, upper panels) the low pressure system (not shown here) over Cyprus resulted in cyclonic activity that enhanced dust transport from the Sahara and air pollution and moisture transport from central and southern Europe. The cyclonic activity of the 21 September then advected eastwards. The backward trajectories show that air masses reached the CUT-TEPAK station at different times from different sources; air masses carrying dust from Egypt and from Tunisia. The air masses from Egypt started at a lower elevation and were then lifted during transport across the Mediterranean, while the dust from Tunisia was transported over a long distance and at higher elevation. Polluted air masses, originating in continental Europe, reached CUT-TEPAK somewhat later in time. Typically, different air masses from different sources converged over CUT-TEPAK at 1.5 km altitude. Interestingly, dust from the Sahara is mixed with air pollution from Europe over Cyprus and the EM region. During the dust outflow-2 event (Fig. 7, middle panels) dust was emitted as a result of the strong surface winds (not shown) in the Negev and Arabian deserts and then transported to the EM ac-

cording to the pressure gradients in the following days. This is confirmed by the backward trajectories which show the dust pathways. The dust reached Cyprus with the highest concentration on the 28 September. By the 29 September the dust was largely removed from the atmosphere. Typically, Europe is a main source of air pollution that is transported to the EM, usually at higher concentrations than in transport from the Middle East (Lelieveld et al., 2002). As a result, the Saharan dust outflow is more strongly mixed with, and subsequently chemically aged by European air pollution, compared to the Arabian dust outflow.

3.3.1 Dynamical and vertical structure (EMAC results)

In the outflow-1 class of events, dust is typically transported from the Sahara to the Mediterranean and then to the EM by Sharav cyclones (Goudie and Middleton, 2006; Ganor et al., 2010), associated with a cold front and often accompanied by rain (Alpert and Ganor, 1993). The model indeed simulates such a frontal system that carries the dust from the Sahara to the EM region (Fig. 8). Velocity vectors are shown at the elevation where the maximum dust concentrations occur during transport. The vertical cross sections at the latitude of the CUT-TEPAK station show the vertical extend of the dust outflow with a maximum concentration at 2.5 km a.s.l. (above sea level). As shown in the figure, the dust moved eastward at this elevation and the dust loading is significantly reduced as the frontal system passed through. The model simulation further shows that the dust is efficiently removed by the precipitation event on 22 September between 06:00 and 15:00 LT, which will be described in more detail below. For the dust outflow-2 event, Fig. 9 shows time series with enhanced dust loading over the EM region. The main dust source is located in the Negev and northern Saudi Arabian deserts, with additional dust originating in the eastern Sinai in Egypt. As a result of the strong surface winds during this period, dust was emitted from this area and transferred to the EM at about 2.5 km altitude a.s.l. in the following days. As shown in Fig. 9, the dust reaches Cyprus with the highest concentration on the 28 September. The cross sections show that the dust is lifted up as high as 6 km altitude with a mass concentration of 1 $\mu g\, m^{-3}$, compared to the maximum height of 2.5 km (same concentration level) in the outflow-1 event. This could result from the prevailing subsidence over the Mediter-

ranean, which prevents the Saharan dust from penetrating to higher altitudes. In contrast, the outflow-2 event is accompanied with strong convective activity over the Middle East deserts, which lifted the dust to higher altitudes. The cross sections in Fig. 9 show that the dust transport from the Middle East occurred at higher elevation than that from the Sahara.

3.3.2 EMAC versus ground based LIDAR profiles

The vertical structure of the dust outflow-2 is compared to ground based LIght Detection And Ranging (LIDAR) measurements of the Cyprus University of Technology (CUT) in Limassol, Cyprus, which also hosts the AERONET station. The LIDAR observations have been recently used to study dust outflows over the EM, including the dust outflow-2 considered in our study (Mamouri et al., 2013; Nisantzi et al., 2014; Mamouri and Ansmann, 2014, 2015) . For a consistent comparison, the LIDAR observations are averaged within the model vertical grid box.

Fig. 10 shows the simulated and observed total and dust only extinction at CUT-TEPAK. The model results are shown at three different longitudes: 33° E at CUT-TEPAK (EMAC), 34° E (EMAC-1) and 35° E (EMAC-2), with all longitudes referring to the latitude of the CUT-TEPAK station (34.675° N). The comparison shows that EMAC captures the LIDAR signal, but 2° (about 200 km) more to the east. This underestimation decreases with each profile further east, indicating a steep gradient of the model dust layer concentration that is associated with the front of the dust-outflow-2 (shown in Fig. 6 and 7). Although the magnitude of the model extinction is predicted lower at the CUT-TEPAK station at both days, EMAC captures the observed peak at 1.5 km height (second day) with a 1.8 km dust layer peak height well, given the relatively coarse vertical grid resolution of the model (which is 500 m at that height).

Interestingly, the calculated vertical extent of the dust layer is wider than the LIDAR signal, which indicates that the total aerosol layer is thicker, at least a few hundred kilometers eastward. This might be related to flow disturbance by the orography, and/or a result of the contribution of other compounds that are considered in our model simulation. The vertically

integrated dust extinction is similar to the total extinction profiles for both EAMC and the observations, but the predicted concentration maximum of the dust layer is closer to the observations for the second day. For the first day, EMAC does not capture the observed dust signal, but the total AOD (integral of the area under the profile) is comparable to the AERONET AOD shown in Fig. 4 for both days.

3.3.3 EMAC vs. CALIPSO retrieved vertical structure

To study the vertical structure of the dust outflow-1 event, the Cloud-Aerosol Lidar and Infrared Pathfinder Satellite Observation (CALIPSO) Level 2 version 3.01, 5 km aerosol profile (APro-Prov) product is used. Unfortunately, no CALIPSO data are available for the outflow-2 case. CALIPSO is a space-borne LIDAR instrument that provides 2-D vertical distributions of atmospheric aerosols at 5 km horizontal resolution and 30–180 m vertical resolution. CALIPSO data retrievals discriminate aerosol layers from clouds and categorizes the particles according to six subtypes (dust, marine, smoke, polluted dust, polluted continental and clean continental), while the observations show the best agreement with AERONET products for dust dominated region (Schuster et al., 2012). Regardless of the CALIPSO uncertainties in retrieving different dust cases, the correlation coefficients are with about 0.58 higher compared to the other aerosol types (Schuster et al., 2012). In addition, the CALIPSO aerosol type classification could overestimate the extinction and the optical depth for marine aerosols. This may add artifacts to the mixed dust classification over land (Kanitz et al., 2014) . Therefore, the CALIPSO data is particularly useful to study the vertical distribution and transport of atmospheric dust (Liu et al., 2008; Uno et al., 2011; Su and Toon, 2011; Johnson et al., 2012). The EMAC calculated dust concentrations and the corresponding extinction are interpolated in space and time to the CALIPSO tracks.

Figure 11 shows two CALIPSO tracks, following the satellite overpass time from left to right. The overpass time is shown in the track name in the upper left corner of each figure. Also included in the upper panels are the scatter plot comparisons between modeled and observed dust extinction, colored by the height of each observation point. In the main figures, the solid black contours represent the modeled dust extinction and the colored

areas represent the CALIPSO extinction observations. The upper panels show the extinction of dust only from both model and CALIPSO, the lower panels include the extinction of all aerosols excluding dust (brown-dotted line), the dust extinction (black line) and the CALIPSO aerosol subtype and cloud classifications. Referring to the upper panel of Fig. 11, the model captures the spatial variability, i.e., the horizontal and vertical extents of the dust plume in both tracks. In particular the height of the dust plume is captured well by the model, which is a critical parameter for determining the dust lifetime in the atmosphere (Levin et al., 2005). The scatter plot shows that the model somewhat underestimates the dust extinction at higher altitudes and overestimates it at lower altitudes. The best agreement is found at the peak concentration of the dust plume, between 2000–3000 m.

For ~~this case, both~~ both cases, the model and ~~the CALIPSO~~ CALISPO results show that ~~dust was removed during transport from the atmosphere by wet and dry deposition, since~~ the dust concentration decreased during the transport and the height of the dust plume ~~decreases from about 4000m~~ decreased from about 4000m over the central Mediterranean on 21 September to about ~~2000m~~ 2000m over the EM on 22 September. ~~This is also confirmed by the independent LIDAR ground observations at CUT-TEPAK station (Mamouri et al., 2013)~~ The model results showed that the dust loading has significantly reduced after the frontal system has passed (Fig. 8) which enhanced the dust deposition (see next section). Concerning the aging of the dust particles during transport, the model and CALIPSO results indicate less interaction between aerosol types and dust aging over North Africa compared to the Mediterranean, where usually stronger mixing between dust and air pollution occurs. This is indicated by many studies (Levin et al., 1996, 2005; Lelieveld et al., 2002). Air pollution in the EM consists of aerosol precursor gases (such as sulfuric, hydrochloric and nitric acid, ammonia) which can directly condense or form semi-volatile compounds on the dust surface (Metzger et al., 2006). The degree of dust aging is indicated by the differences between the black and brown-dotted contour lines, and by the CALIPSO classifications. Over the Mediterranean, from latitudes higher than 30° N, aging of dust is observed from both model (black and brown-dotted contours) and CALIPSO classifications (which subsequently shows smoke, polluted dust, polluted

continental). The CALIPSO classification "polluted dust" may cover cases where dust is mixed with other aerosols, but not necessarily chemically aged. With the current CALIPSO version 3.01 algorithm, it is not possible to distinguish between dust mixing and dust aging by air pollution. In such cases, polluted dust may represent aged dust. The comparison with our model results can help distinguish between the types of aerosol extinction.

3.3.4 Dust removal

To evaluate the dust scavenging and precipitation over the EM we use the Tropical Rainfall Measuring Mission (TRMM) level-3 (collection 3B42) 3 hourly product (http://pmm.nasa.gov/TRMM). Figure 12 shows the time evolution of the dust removal by wet and dry deposition mechanisms as well as the total dust removal at the surface. The blue contours show the TRMM precipitation observations at the surface with the modeled dust removed by wet scavenging overlaid. As shown in the figure, starting from 20 September, the dust was mainly removed by scavenging associated with strong precipitation. The precipitation events started on 20 September from 20 up to 40° E. The figure shows that the calculated dust wet scavenging largely coincides with the observed precipitation; however the model may overestimate wet scavenging of the dust. Dry removal was insignificant for the dust outflow-1 event. On 23 September the dust concentration decreased over the area from 35 to 50° E as a result of dilution during the dissolution of the low pressure system developed over the region. In the outflow-2 event the dust was largely removed from 26 September onward, which explains the increase of the dust concentration at the surface due to particle sedimentation from elevations above 2 km. The efficiency of the dust wet scavenging depends strongly on the aged dust fraction; by increasing the soluble dust fraction the dust wet scavenging increases, since aged dust particles can be more efficiently taken up by cloud droplets (Teller et al., 2012). This is captured by our model set up which employs the comprehensive scavenging mechanism of Tost et al. (2006).

3.4 Dust removal sensitivity to dust aging

During the outflow-1 event the dust is efficiently removed by precipitation over the EM as a result of mixing of African dust with air pollution from Europe. This results in reduction of the AOD from 0.5 to 0.05 at the ATHENS-NOA station (Fig. 4). To study the impact of dust aging on the removal efficiency, it was switched off in a sensitivity simulation for which the condensation of soluble compounds on dust particles has been excluded. This results in dust wet removal by impaction scavenging only, while nucleation scavenging is not considered (Tost et al., 2006). Figure 13 shows the time evolution of dust wet removal for the aged and non-aged (hence pristine) dust cases at cross-sections passing over two different stations, ATHENS-NOA and CUT-TEPAK. The TRMM precipitation observations are overlaid. The right panels of the figures show the differences between the wet dust removal at the surface for both cases. The TRMM precipitation and dust removal in Fig. 13 differs from Fig. 12 as a result of different model resolutions (T106 and T255, respectively). The differences in the TRMM precipitation between Figs. 12 and 13 results from regridding of the TRMM precipitation (25 km resolution) to the model resolution (50 and 110 km). The dust removal by the higher model resolution, Fig. 12, resolves the observations better in space and time (note the slightly different time axis to focus on the dust outflow-1 event).

Figure 13 shows that the dust wet removal is simulated realistically in space and time at both stations, compared to the TRMM observations. The aged and non-aged cases show significant difference in the dust wet removal. Obviously, an additional amount of the dust is removed due to aging processes (EMAC results) as a result of mixing with air pollution from Europe. The average difference in the wet dust removal is $10\,\mathrm{mg\,m^{-2}}$ at ATHENS-NOA and twice as much dust is removed in the case of aging. At CUT-TEPAK, the dust concentration in the atmosphere is lower due to removal processes during transport, and also because of less precipitation compared to the TRMM observations at ATHENS-NOA. This results in stronger dust wet removal at ATHENS-NOA than at CUT-TEPAK. Figure 14 shows the total time integral of the dust removal for CUT-TEPAK and ATHENS-NOA as shown in Fig. 13. The total dust removal for the case of aging (labeled “EMAC”) is generally higher than by

switching off the aging (labeled "NoAging"). This effect is more pronounced for the wet removal than for the dry deposition. Dry removal is enhanced in the case of aging due to the condensation of additional soluble compounds on the originally insoluble dust particles, which increases their size and weight and shifts them to the soluble mode. This inter-modal shift results in higher wet removal by the subsequent nucleation scavenging. In EMAC, the latter acts on dust particles which are only in the soluble mode and which are, if present, by definition aged (in our set-up). In contrast to the dry deposition, the ratios between the aging and non-aging cases are much higher for ATHENS-NOA than for CUT-TEPAK, which is mainly a result of the different dust loadings. As a result, the difference between the aged and non-aged is less significant at CUT-TEPAK compared to ATHENS-NOA. This suggests that during the transport from Africa to the EM region, aging largely determines the dust and air pollution lifetime over the EM.

3.5 Aged Dust Proxy (ADP)

To identify the dust-air pollution interactions, back trajectories of various model aerosol concentrations have been sampled along HYSPLIT back trajectories for both dust outflow cases, i.e., sulfuric, nitric and hydrochloric acid, insoluble coarse mode dust (DU_ci) as shown in Fig. 15. For the dust outflow-1 event four trajectories are calculated (trajectory Traj-1 to Traj-4), which represent the air masses arriving from the Sahara and Europe. For the dust outflow-2 event air masses originated over the Negev and Arabian deserts, as shown by trajectories Traj-5 toTraj-8. Different colors refer to the concentrations, while the marker types refer to different trajectories. Additionally shown is the ratio between the coarse mode soluble (DU_cs) and insoluble (DU_ci) dust mass fraction, which can be regarded as an aged dust proxy (ADP). The ADP is introduced to illustrate the aging mechanism in EMAC. In our EMAC aerosol set up, dust is originally emitted only in the insoluble accumulation (DU_ai) and coarse mode (DU_ci). Upon aging, which requires the condensation of strong acids, the aged dust fraction is transferred to the corresponding soluble mode, e.g., DU_ai to DU_as and DU_ci to DU_cs, whereby DU_as can further grow into DU_cs, as a result of aerosol hygroscopic growth or coagulation (Pringle et al., 2010). Thus, a low ADP indicates

freshly emitted dust which is not aged, while high ADP values indicate aged dust. For very high ADP values, dust has been subject to long-range transport with significant aging, since practically all insoluble dust has been transferred into the soluble mode. This is the case north and west of Cyprus, where dust becomes strongly polluted during both dust events.

The dust concentration shows an increasing tendency along the trajectories Traj-1 and Traj-2 as they reach Cyprus. This results from the actual dust supply from the dust emission sources along Traj-2, which originates in Libya. Trajectories Traj-3 and Traj-4, which originate in Europe, show very low dust concentrations, due to the absence of dust emission sources in southern Europe (in EMAC). However, the trajectories of sulfuric and nitric acid show instead an increasing tendency along Traj-3 and Traj-4. The low pressure system over Cyprus during the 2nd dust event enhanced the transport of different aerosols and gases to the EM. The relatively low wind speed within the low pressure system, shown in Fig. 9, increased the residence time of pollution and dust, and allowed extended mixing and efficient dust aging. As a result, dust particles have been successively coated by different soluble compounds, which increases the ADP over time as the air masses approach Cyprus from the west (Traj-1 to Traj-4). Note that the ADP is higher for Traj-3 and Traj-4 due to the lower insoluble dust (DU_ci) concentration along these trajectories compared to Traj-1 and Traj-2. For the dust outflow-2 event, the ADP is much lower compared to the outflow-1 event since the dust does not encounter much air pollution from Europe and thus less effectively ages. Interestingly, as long as the sulfuric and nitric acid concentrations increase along Traj-5 to Traj-8 over the Mediterranean, the ADP increases from about 1 to 13. This underscores the strong interaction between the dust and air pollution over the EM due to the relatively high air pollution concentrations.

4 Conclusions

Interactions of dust and air pollution over the EM have been studied, focusing on two distinct dust transport events on 22 and 28 September 2011, using the atmospheric chemistry – climate model EMAC at relatively high spectral resolution (T255L31, about 50 km grid

spacing). At lower resolution (T106L31, about 110 km grid spacing), in an extended 2 year simulation (2010–2011), the model performs reasonably well in simulating the PM and AOD over the EM, while at high resolution the model results closely agree with the observations. Concentrations of calcium cations, used as a proxy for dust reactivity, show good agreement with ground-based observations. The model captures the AOD at different AERONET stations in the region, however, with some underestimation at the CUT-TEPAK station in Cyprus, coincident with relatively strong aging and efficient removal of the dust.

Both, simulation results and backward trajectory analysis show that the development of a synoptic low pressure system over the EM enhances the dust transport from the Sahara along the cold front, which also carries dust from the Negev and Arabian deserts as well as air pollution to the EM. The model reproduces the frontal system and the associated precipitation. Our results show that the Saharan dust was mainly removed by precipitation, which is captured well by the model, consistent with observations. Generally, EMAC captures the dust transport in both cases, and the vertical structure of dust layers is reproduced accurately by the model, confirmed by CALISPO satellite observations. Also the mixing of dust with air pollution over the EM is captured well by the model compared to the CALIPSO observations and aerosol classifications. Both, EMAC and CALIPSO show that the mixing between dust and air pollution can be very efficient over the Mediterranean.

The model results indicate that the dust is ~~rapidly~~ aged, especially from the Sahara and to a lesser degree from the Negev and Arabian deserts. The level of aging depends mainly on the mixing time between dust and air pollution and concentrations of the latter. The longer travel period for Saharan dust therefore results in more efficient aging compared to Arabian dust arriving in the EM, illustrated by a newly introduced aged dust proxy. Based on a sensitivity study we find that the mixing of air pollution and dust enhances nucleation scavenging, resulting in three times more rapid dust scavenging compared to non-aged (pristine) dust, while uptake of pollution and consequent hygroscopic growth also enhances sedimentation and dry deposition. Our study suggests that the aging of dust over the EM can significantly decrease the dust lifetime and atmospheric loading.

Acknowledgements. All simulations in this study were carried out on the Cy-Tera Cluster. The Project Cy-Tera (NEA-$Y\Pi O\Delta OMH/\Sigma TPATH$/0308/31) is co-financed by the European Regional Development Fund and the Republic of Cyprus through the Research Promotion Foundation. The research leading to these results has received funding from the European Research Council under the European Union's Seventh Framework Program (FP7/2007-2013) / ERC grant agreement no 226144. The authors thank the NASA AERONET team for providing the AERONET data used in this study and the team of Mr. Savvas Kleathous, Cyprus Ministry of Labour and Social Insurance, for providing the sulfate, calcium and PM observations at Agia Marina station (Cyprus). The authors thank the Remote sensing and Geo-Environment Research laboratory of Cyprus University of Technology (CUT) for providing the LIDAR extinction profiles at the CUT-TEPAK station.

References

Alpert, P. and Ganor, E.: A jet stream associated heavy dust storm in the western Mediterranean, J. Geophys. Res., 98, 7339, doi:10.1029/92JD01642, 1993.

Ardon-Dryer, K. and Levin, Z.: Ground-based measurements of immersion freezing in the eastern Mediterranean, Atmos. Chem. Phys., 14, 5217–5231, doi:10.5194/acp-14-5217-2014, 2014.

Astitha, M., Kallos, G., Spyrou, C., O'Hirok, W., Lelieveld, J., and Denier van der Gon, H. A. C.: Modelling the chemically aged and mixed aerosols over the eastern central Atlantic Ocean — potential impacts, Atmos. Chem. Phys., 10, 5797–5822, doi:10.5194/acp-10-5797-2010, 2010.

Astitha, M., Lelieveld, J., Abdel Kader, M., Pozzer, A., and de Meij, A.: Parameterization of dust emissions in the global atmospheric chemistry-climate model EMAC: impact of nudging and soil properties, Atmos. Chem. Phys., 12, 11057–11083, doi:10.5194/acp-12-11057-2012, 2012.

Bauer, S. E., Balkanski, Y., Schulz, M., Hauglustaine, D. A., and Dentener, F.: Global modeling of heterogeneous chemistry on mineral aerosol surfaces: influence on tropospheric ozone chemistry and comparison to observations, J. Geophys. Res.-Atmos., 109, D02304, doi:10.1029/2003JD003868, 2004.

Bauer, S. E., Mishchenko, M. I., Lacis, A. A., Zhang, S., Perlwitz, J., and Metzger, S. M.: Do sulfate and nitrate coatings on mineral dust have important effects on radiative properties and climate modeling?, J. Geophys. Res., 112, D0630, doi:10.1029/2005JD006977, 2007.

Crowley, J. N., Ammann, M., Cox, R. A., Hynes, R. G., Jenkin, M. E., Mellouki, A., Rossi, M. J., Troe, J., and Wallington, T. J.: Evaluated kinetic and photochemical data for atmospheric chem-

istry: Volume V – heterogeneous reactions on solid substrates, Atmos. Chem. Phys., 10, 9059–9223, doi:10.5194/acp-10-9059-2010, 2010.

Dayan, U., Heffter, J., Miller, J., and Gutman, G.: Dust intrusion events into the Mediterranean Basin, J. Appl. Meteorol., 30, 1185–1199, doi:10.1175/1520-0450(1991)030<1185:DIEITM>2.0.CO;2, 1991.

Dayan, U., Ziv, B., Shoob, T., and Enzel, Y.: Suspended dust over southeastern Mediterranean and its relation to atmospheric circulations, Int. J. Climatol., 28, 915–924, doi:10.1002/joc.1587, 2008.

de Meij, A. and Lelieveld, J.: Evaluating aerosol optical properties observed by ground-based and satellite remote sensing over the Mediterranean and the Middle East in 2006, Atmos. Res., 99, 415–433, doi:10.1016/j.atmosres.2010.11.005, 2011.

de Meij, A., Pozzer, A., Pringle, K., Tost, H., and Lelieveld, J.: EMAC model evaluation and analysis of atmospheric aerosol properties and distribution with a focus on the Mediterranean region, Atmos. Res., 114–115, 38–69, doi:10.1016/j.atmosres.2012.05.014, 2012.

Dentener, F. J., Carmichael, G. R., Zhang, Y., Lelieveld, J., and Crutzen, P. J.: Role of mineral aerosol as a reactive surface in the global troposphere, J. Geophys. Res., 101, 22869, doi:10.1029/96JD01818, 1996.

Fountoukis, C. and Nenes, A.: ISORROPIA II: a computationally efficient thermodynamic equilibrium model for K^+–Ca^{2+}–Mg^{2+}–NH_4^+–Na^+–SO_4^{2-}–NO_3^-–Cl^-–H_2O aerosols, Atmos. Chem. Phys., 7, 4639–4659, doi:10.5194/acp-7-4639-2007, 2007.

Fuchs, N. A. and Davies, C. N.: The mechanics of aerosols, Dover Publications, New York, 1989.

Ganor, E. and Mamane, Y.: Transport of Saharan dust across the eastern Mediterranean, Atmos. Environ., 16, 581–587, doi:10.1016/0004-6981(82)90167-6, 1982.

Ganor, E., Osetinsky, I., Stupp, A., and Alpert, P.: Increasing trend of African dust, over 49 years, in the eastern Mediterranean, J. Geophys. Res., 115, D07201, doi:10.1029/2009JD012500, 2010.

Gläser, G., Kerkweg, A., and Wernli, H.: The Mineral Dust Cycle in EMAC 2.40: sensitivity to the spectral resolution and the dust emission scheme, Atmos. Chem. Phys., 12, 1611–1627, doi:10.5194/acp-12-1611-2012, 2012.

Goudie, A. and Middleton, N.: Desert Dust in the Global System, Springer, Berlin, New York, 292, 2006.

Holben, B., Eck, T., Slutsker, I., Tanré, D., Buis, J., Setzer, A., Vermote, E., Reagan, J., Kaufman, Y., Nakajima, T., Lavenu, F., Jankowiak, I., and Smirnov, A.: AERONET – a federated instrument network and data archive for Aerosol characterization, Remote Sens. Environ., 66, 1–16, doi:10.1016/S0034-4257(98)00031-5, 1998.

Jöckel, P., Kerkweg, A., Pozzer, A., Sander, R., Tost, H., Riede, H., Baumgaertner, A., Gromov, S., and Kern, B.: Development cycle 2 of the Modular Earth Submodel System (MESSy2), Geosci. Model Dev., 3, 717–752, doi:10.5194/gmd-3-717-2010, 2010.

Johnson, M. S., Meskhidze, N., and Praju Kiliyanpilakkil, V.: A global comparison of GEOS-Chem-predicted and remotely-sensed mineral dust aerosol optical depth and extinction profiles, J. Adv. Model. Earth Syst, 4, M07001, doi:10.1029/2011MS000109, 2012.

Kallos, G., Papadopoulos, A., Katsafados, P., and Nickovic, S.: Transatlantic Saharan dust transport: model simulation and results, J. Geophys. Res., 111, D09204, doi:10.1029/2005JD006207, 2006.

Kanitz, T., Ansmann, A., Foth, A., Seifert, P., Wandinger, U., Engelmann, R., Baars, H., Althausen, D., Casiccia, C., and Zamorano, F.: Surface matters: limitations of CALIPSO V3 aerosol typing in coastal regions, Atmospheric Measurement Techniques, 7, 2061–2072, doi:10.5194/amt-7-2061-2014, http://www.atmos-meas-tech.net/7/2061/2014/, 2014.

Koop, T. and Mahowald, N.: Atmospheric science: the seeds of ice in clouds, Nature, 498, 302–303, doi:10.1038/nature12256, 2013.

Lelieveld, J., Berresheim, H., Borrmann, S., Crutzen, P. J., Dentener, F. J., Fischer, H., Feichter, J., Flatau, P. J., Heland, J., Holzinger, R., Korrmann, R., Lawrence, M. G., Levin, Z., Markowicz, K. M., Mihalopoulos, N., Minikin, A., Ramanathan, V., de Reus, M., Roelofs, G. J., Scheeren, H. A., Sciare, J., Schlager, H., Schultz, M., Siegmund, P., Steil, B., Stephanou, E. G., Stier, P., Traub, M., Warneke, C., Williams, J., and Ziereis, H.: Global air pollution crossroads over the Mediterranean, Science, 298, 794–799, doi:10.1126/science.1075457, 2002.

Levin, Z., Ganor, E., and Gladstein, V.: The effects of desert particles coated with sulfate on rain formation in the Eastern Mediterranean, J. Appl. Meteorol., 35, 1511–1523, doi:10.1175/1520-0450(1996)035<1511:TEODPC>2.0.CO;2, 1996.

Levin, Z., Teller, A., Ganor, E., and Yin, Y.: On the interactions of mineral dust, sea-salt particles, and clouds: a measurement and modeling study from the Mediterranean Israeli Dust Experiment campaign, J. Geophys. Res.-Atmos., 110, D20202, doi:10.1029/2005JD005810, 2005.

Liu, Z., Omar, A., Vaughan, M., Hair, J., Kittaka, C., Hu, Y., Powell, K., Trepte, C., Winker, D., Hostetler, C., Ferrare, R., and Pierce, R.: CALIPSO lidar observations of the optical properties of Saharan dust: a case study of long-range transport, J. Geophys. Res., 113, D07207, doi:10.1029/2007JD008878, 2008.

Mahowald, N. M., Engelstaedter, S., Luo, C., Sealy, A., Artaxo, P., Benitez-Nelson, C., Bonnet, S., Chen, Y., Chuang, P. Y., Cohen, D. D., Dulac, F., Herut, B., Johansen, A. M., Kubilay, N., Losno, R., Maenhaut, W., Paytan, A., Prospero, J. M., Shank, L. M., and Siefert, R. L.: Atmospheric iron

deposition: global distribution, variability, and human perturbations, Annu. Rev. Marine Sci., 1, 245–278, doi:10.1146/annurev.marine.010908.163727, 2009.

Mamouri, R. E. and Ansmann, A.: Estimated desert-dust ice nuclei profiles from polarization lidar: methodology and case studies, Atmospheric Chemistry and Physics, 15, 3463–3477, doi:10.5194/acp-15-3463-2015, http://www.atmos-chem-phys.net/15/3463/2015/, 2015.

Mamouri, R. E. and Ansmann, A.: Fine and coarse dust separation with polarization lidar, Atmospheric Measurement Techniques, 7, 3717–3735, doi:10.5194/amt-7-3717-2014, http://www.atmos-meas-tech.net/7/3717/2014/, 2014.

Mamouri, R. E., Ansmann, A., Nisantzi, A., Kokkalis, P., Schwarz, A., and Hadjimitsis, D.: Low Arabian dust extinction-to-backscatter ratio: Arabian dust lidar ratio, Geophys. Res. Lett., 4762–4766, doi:10.1002/grl.50898, 2013.

Manktelow, P. T., Carslaw, K. S., Mann, G. W., and Spracklen, D. V.: The impact of dust on sulfate aerosol, CN and CCN during an East Asian dust storm, Atmos. Chem. Phys., 10, 365–382, doi:10.5194/acp-10-365-2010, 2010.

Metzger, S., Mihalopoulos, N., and Lelieveld, J.: Importance of mineral cations and organics in gas–aerosol partitioning of reactive nitrogen compounds: case study based on MINOS results, Atmos. Chem. Phys., 6, 2549–2567, doi:10.5194/acp-6-2549-2006, 2006.

Mogili, P. K., Kleiber, P. D., Young, M. A., and Grassian, V. H.: Heterogeneous uptake of ozone on reactive components of mineral dust aerosol: an environmental aerosol reaction chamber study, J. Phys. Chem. A, 110, 13799–13807, doi:10.1021/jp063620g, 2006.

Moulin, C., Lambert, C. E., Dayan, U., Masson, V., Ramonet, M., Bousquet, P., Legrand, M., Balkanski, Y. J., Guelle, W., Marticorena, B., Bergametti, G., and Dulac, F.: Satellite climatology of African dust transport in the Mediterranean atmosphere, J. Geophys. Res., 103, 13137, doi:10.1029/98JD00171, 1998.

Nenes, A., Krom, M. D., Mihalopoulos, N., Van Cappellen, P., Shi, Z., Bougiatioti, A., Zarmpas, P., and Herut, B.: Atmospheric acidification of mineral aerosols: a source of bioavailable phosphorus for the oceans, Atmos. Chem. Phys., 11, 6265–6272, doi:10.5194/acp-11-6265-2011, 2011.

Nisantzi, A., Mamouri, R. E., Ansmann, A., and Hadjimitsis, D.: Injection of mineral dust into the free troposphere during fire events observed with polarization lidar at Limassol, Cyprus, Atmospheric Chemistry and Physics, 14, 12 155–12 165, doi:10.5194/acp-14-12155-2014, http://www.atmos-chem-phys.net/14/12155/2014/, 2014.

Papayannis, A., Balis, D., Amiridis, V., Chourdakis, G., Tsaknakis, G., Zerefos, C., Castanho, A. D. A., Nickovic, S., Kazadzis, S., and Grabowski, J.: Measurements of Saharan dust aerosols over

the Eastern Mediterranean using elastic backscatter-Raman lidar, spectrophotometric and satellite observations in the frame of the EARLINET project, Atmos. Chem. Phys., 5, 2065–2079, doi:10.5194/acp-5-2065-2005, 2005.

Pey, J., Querol, X., Alastuey, A., Forastiere, F., and Stafoggia, M.: African dust outbreaks over the Mediterranean Basin during 2001–2011: PM_{10} concentrations, phenomenology and trends, and its relation with synoptic and mesoscale meteorology, Atmos. Chem. Phys., 13, 1395–1410, doi:10.5194/acp-13-1395-2013, 2013.

Pozzer, A., de Meij, A., Pringle, K. J., Tost, H., Doering, U. M., van Aardenne, J., and Lelieveld, J.: Distributions and regional budgets of aerosols and their precursors simulated with the EMAC chemistry-climate model, Atmos. Chem. Phys., 12, 961–987, doi:10.5194/acp-12-961-2012, 2012.

Pringle, K. J., Tost, H., Message, S., Steil, B., Giannadaki, D., Nenes, A., Fountoukis, C., Stier, P., Vignati, E., and Lelieveld, J.: Description and evaluation of GMXe: a new aerosol submodel for global simulations (v1), Geosci. Model Dev., 3, 391–412, doi:10.5194/gmd-3-391-2010, 2010.

Reitz, P., Spindler, C., Mentel, T. F., Poulain, L., Wex, H., Mildenberger, K., Niedermeier, D., Hartmann, S., Clauss, T., Stratmann, F., Sullivan, R. C., DeMott, P. J., Petters, M. D., Sierau, B., and Schneider, J.: Surface modification of mineral dust particles by sulphuric acid processing: implications for ice nucleation abilities, Atmos. Chem. Phys., 11, 7839–7858, doi:10.5194/acp-11-7839-2011, 2011.

Roeckner, E., Brokopf, R., Esch, M., Giorgetta, M., Hagemann, S., Kornblueh, L., Manzini, E., Schlese, U., and Schulzweida, U.: Sensitivity of simulated climate to horizontal and vertical resolution in the ECHAM5 atmosphere model, J. Climate, 19, 3771–3791, doi:10.1175/JCLI3824.1, 2006.

Rosenfeld, D., Rudich, Y., and Lahav, R.: Desert dust suppressing precipitation: a possible desertification feedback loop, P. Natl. Acad. Sci. USA, 98, 5975–5980, doi:10.1073/pnas.101122798, 2001.

Sander, R., Kerkweg, A., Jöckel, P., and Lelieveld, J.: Technical note: The new comprehensive atmospheric chemistry module MECCA, Atmos. Chem. Phys., 5, 445–450, doi:10.5194/acp-5-445-2005, 2005.

Schulz, M., Prospero, J. M., Baker, A. R., Dentener, F., Ickes, L., Liss, P. S., Mahowald, N. M., Nickovic, S., García-Pando, C. P., Rodríguez, S., Sarin, M., Tegen, I., and Duce, R. A.: Atmospheric transport and deposition of mineral dust to the ocean: implications for research needs, Environ. Sci. Technol., 46, 10390–10404, doi:10.1021/es300073u, 2012.

Schuster, G. L., Vaughan, M., MacDonnell, D., Su, W., Winker, D., Dubovik, O., Lapyonok, T., and Trepte, C.: Comparison of CALIPSO aerosol optical depth retrievals to AERONET measurements, and a climatology for the lidar ratio of dust, Atmos. Chem. Phys., 12, 7431–7452, doi:10.5194/acp-12-7431-2012, 2012.

Seinfeld, J. H. and Pandis, S. N.: Atmospheric chemistry and physics: from air pollution to climate change, J. Wiley, Hoboken, N.J., 2006.

Stocker, T. F., Qin, D., Plattner, G. K., Tignor, M., Allen, S. K., Boschung, J., Nauels, A., Xia, Y., Bix, V., and Midgley, P. M.: Climate Change 2013: the Physical Science Basis: Working Group I Contribution to the Fifth Assessment Report of the Intergovernmental Panel on Climate Change, Cambridge University Press, New York, 2014.

Su, L. and Toon, O. B.: Saharan and Asian dust: similarities and differences determined by CALIPSO, AERONET, and a coupled climate-aerosol microphysical model, Atmos. Chem. Phys., 11, 3263–3280, doi:10.5194/acp-11-3263-2011, 2011.

Taylor, K. E.: Summarizing multiple aspects of model performance in a single diagram, J. Geophys. Res., 106, 7183, doi:10.1029/2000JD900719, 2001.

Teller, A., Xue, L., and Levin, Z.: The effects of mineral dust particles, aerosol regeneration and ice nucleation parameterizations on clouds and precipitation, Atmos. Chem. Phys., 12, 9303–9320, doi:10.5194/acp-12-9303-2012, 2012.

Tost, H., Jöckel, P., Kerkweg, A., Sander, R., and Lelieveld, J.: Technical note: A new comprehensive SCAVenging submodel for global atmospheric chemistry modelling, Atmos. Chem. Phys., 6, 565–574, doi:10.5194/acp-6-565-2006, 2006.

Tost, H., Lawrence, M. G., Brühl, C., Jöckel, P., The GABRIEL Team, and The SCOUT-O3-DARWIN/ACTIVE Team: Uncertainties in atmospheric chemistry modelling due to convection parameterisations and subsequent scavenging, Atmos. Chem. Phys., 10, 1931–1951, doi:10.5194/acp-10-1931-2010, 2010.

Trebs, I., Metzger, S., Meixner, F. X., Helas, G., Hoffer, A., Rudich, Y., Falkovich, A. H., Moura, M. A. L., da Silva, R. S., Artaxo, P., Slanina, J., and Andreae, M. O.: The NH_4^+ – NO_3^- – Cl^- – SO_4^{2-} – H_2O aerosol system and its gas phase precursors at a pasture site in the Amazon Basin: how relevant are mineral cations and soluble organic acids?, J. Geophys. Res.-Atmos., 110, D07303, doi:10.1029/2004JD005478, 2005.

Uno, I., Eguchi, K., Yumimoto, K., Liu, Z., Hara, Y., Sugimoto, N., Shimizu, A., and Takemura, T.: Large Asian dust layers continuously reached North America in April 2010, Atmos. Chem. Phys., 11, 7333–7341, doi:10.5194/acp-11-7333-2011, 2011.

van der Werf, G. R., Randerson, J. T., Giglio, L., Collatz, G. J., Mu, M., Kasibhatla, P. S., Morton, D. C., DeFries, R. S., Jin, Y., and van Leeuwen, T. T.: Global fire emissions and the contribution of deforestation, savanna, forest, agricultural, and peat fires (1997–2009), Atmos. Chem. Phys., 10, 11707–11735, doi:10.5194/acp-10-11707-2010, 2010.

Yin, Y., Wurzler, S., Levin, Z., and Reisin, T. G.: Interactions of mineral dust particles and clouds: effects on precipitation and cloud optical properties, J. Geophys. Res.-Atmos., 107, 4724, doi:10.1029/2001JD001544, 2002.

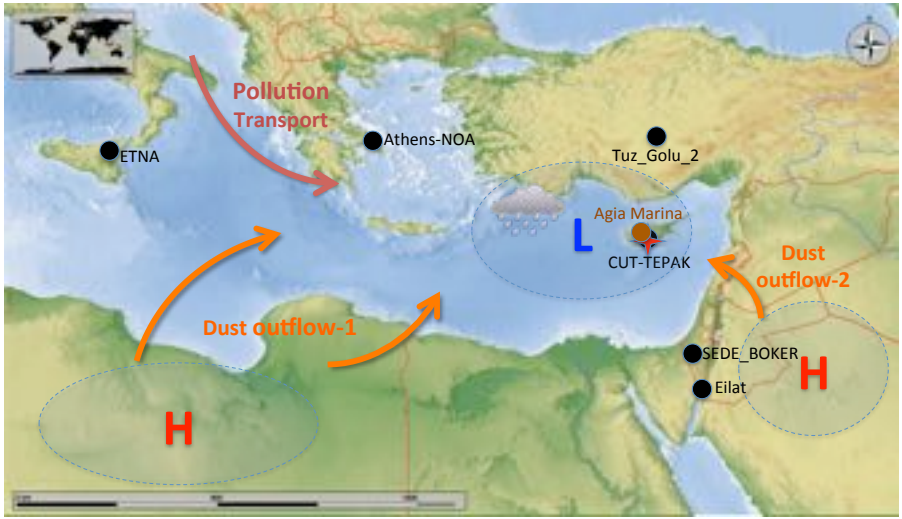

Figure 1. Schematic representation of the prevailing synoptic conditions. Cyprus low, main transport pathways for dust (orange) and air pollution (red) during both dust outflow event to the EM. Observational stations are included: AERONET (black), EMEP station Agia Marina (brown).

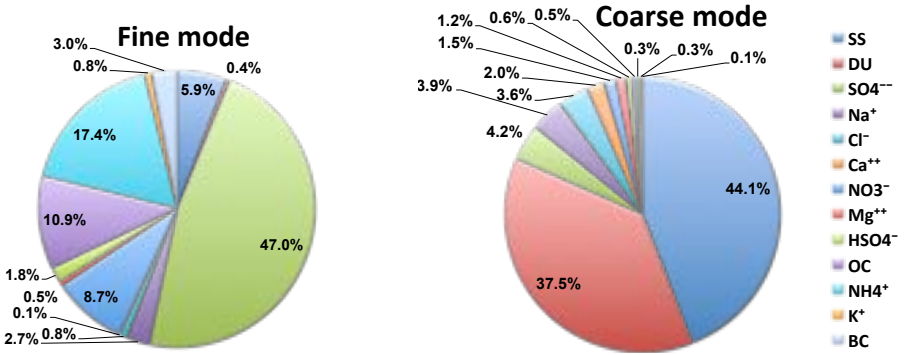

Figure 2. Aerosol mass fractions based on two years of model results for CUT-TEPAK in Cyprus.

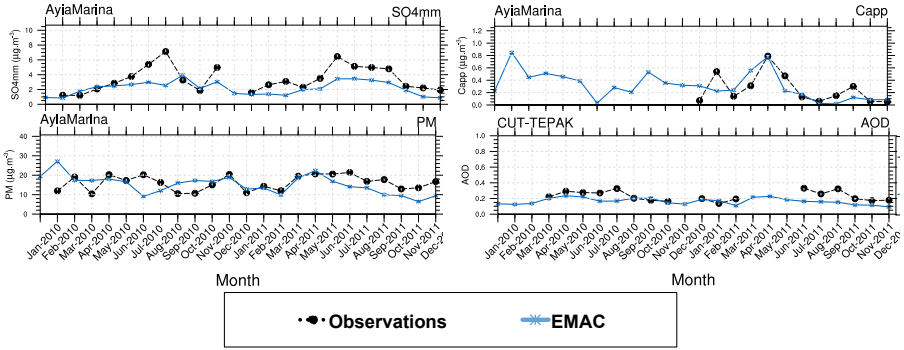

Figure 3. EMAC (T106L31) results (blue line): Aerosol sulfate (SO_4^{2-}), calcium (Ca^{2+}), total particulate (dry) matter (PM) and AOD (550 nm) compared to observations (black circles) at the EMEP station Ayia Marina and the AERONET station CUT-TEPAK in Cyprus, 2010–2011 (monthly means).

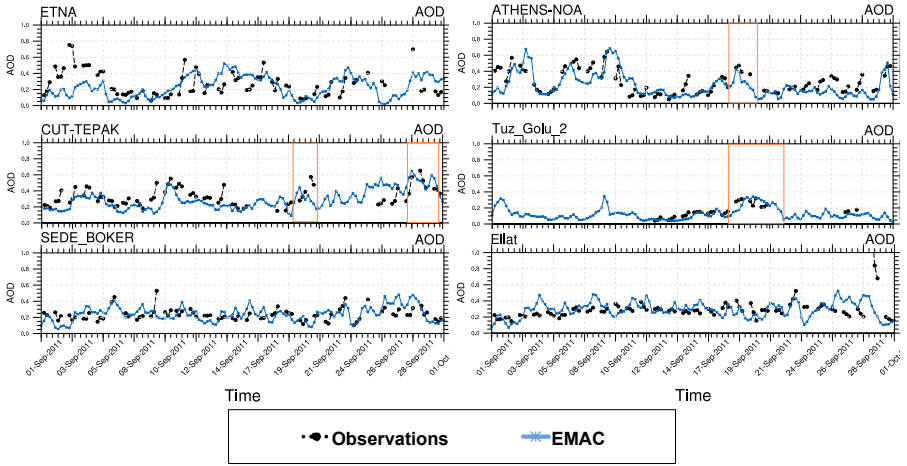

Figure 4. EMAC (T255L31) model results (blue line) of AOD (550 nm) and AERONET observations (black dots). The orange boxes delineate the dust outflow events.

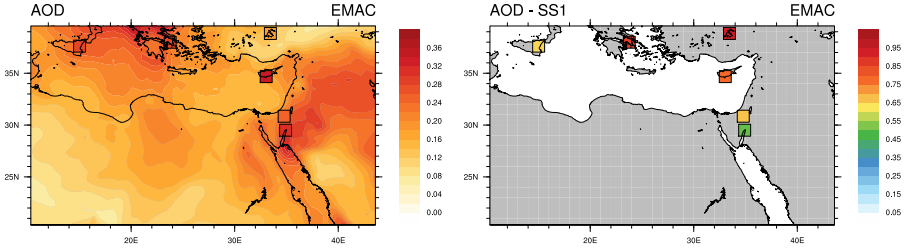

Figure 5. EMAC (T255L31) model results of AOD (550 nm) for September 2011 (left) and skill score (right). The six AERONET stations of Fig. 4 are included (squares).

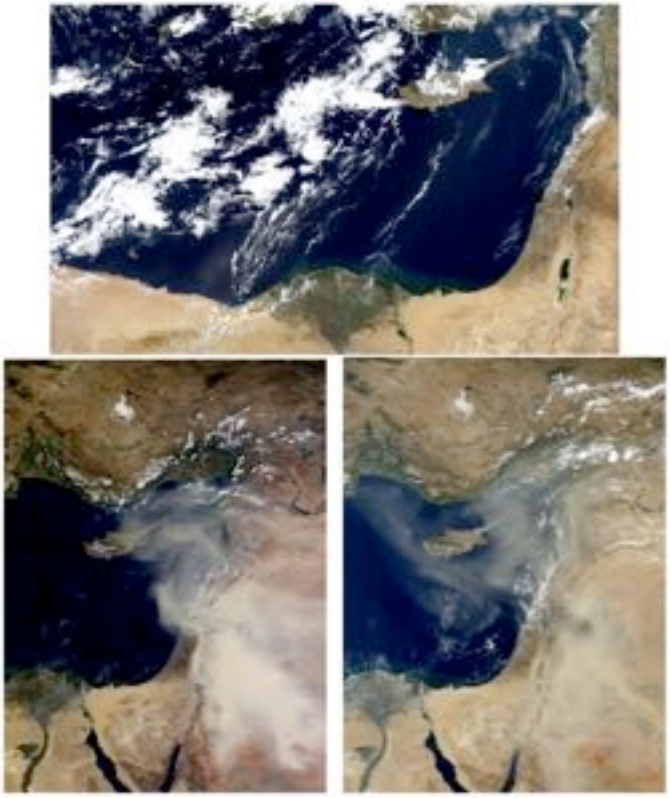

Figure 6. MODIS-Aqua true color image (top) for 22 September (11:10 UTC overpass time) with clouds and dust outflow from Libya to the EM. (Bottom) MODIS-Terra true color images: (left) 28 September 2011 (08:55 UTC overpass time), (right) 29 September 2011 (08:00 UTC overpass time) with dust outflow from the Negev and Arabian deserts to the EM.

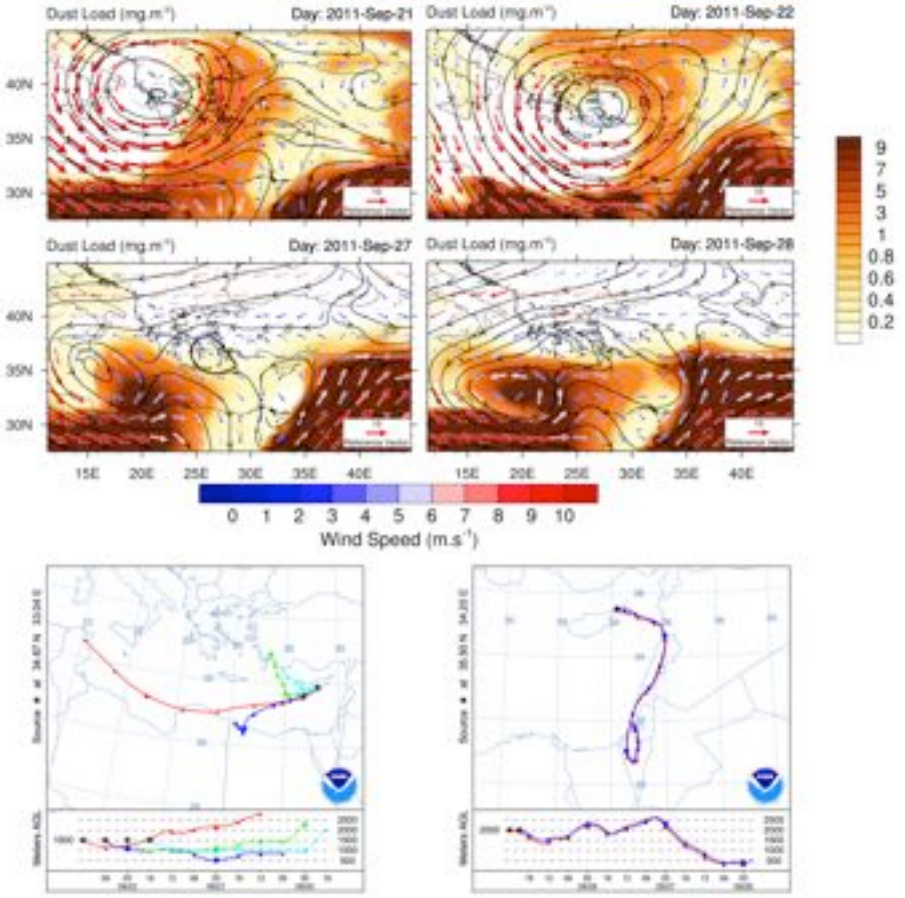

Figure 7. Daily average dust load over the Eastern Mediterranean and HYSPLIT model backward trajectories ending at 12:00 UTC 22 September at the CUT-TEPAK station and 21:00 on 28 September 2011 at 35.5° N and 34.3° E for both dust outflow events.

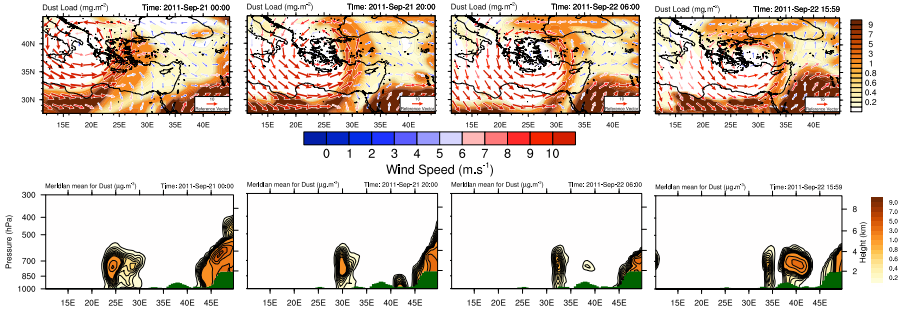

Figure 8. Time series of (top) dust load and (bottom) ~~vertical cross-sections at the CUT-TEPAK station~~ meridional mean for the first event ~~, the~~ at CUT-TEPAK location (34.675° N). The green shaded area represents the orography.

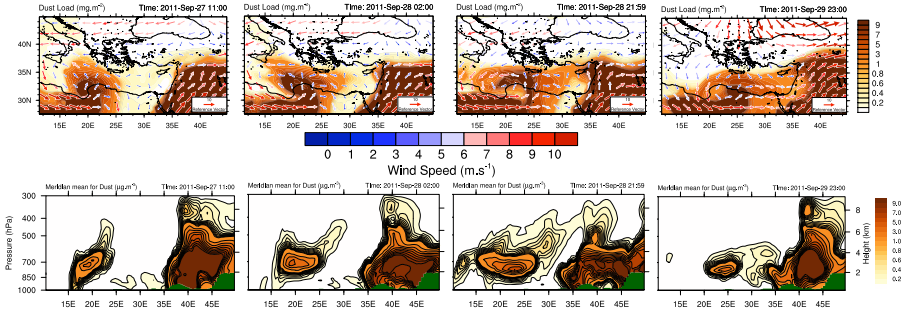

Figure 9. Time series of (top) dust load and (bottom) ~~vertical cross-sections at the CUT-TEPAK station~~ meridional mean for the second event ~~, the~~ at CUT-TEPAK location (34.675° N). The green shaded area represents the orography.

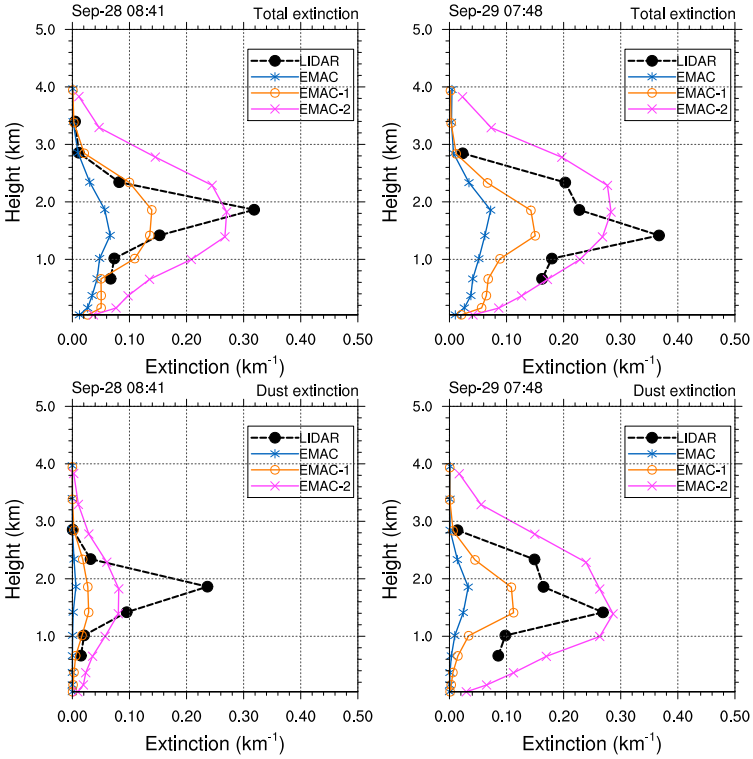

Figure 10. Comparison between the modeled and the observed total and dust only extinction coefficient at CUT-TEPAK LIDAR station at different longitudes: 33 °E (EMAC) at CUT-TEPAK station, 34°E (EMAC-1) and 35°E (EMAC-2); all longitudes refer to the latitude of CUT-TEPAK (34.675°N).

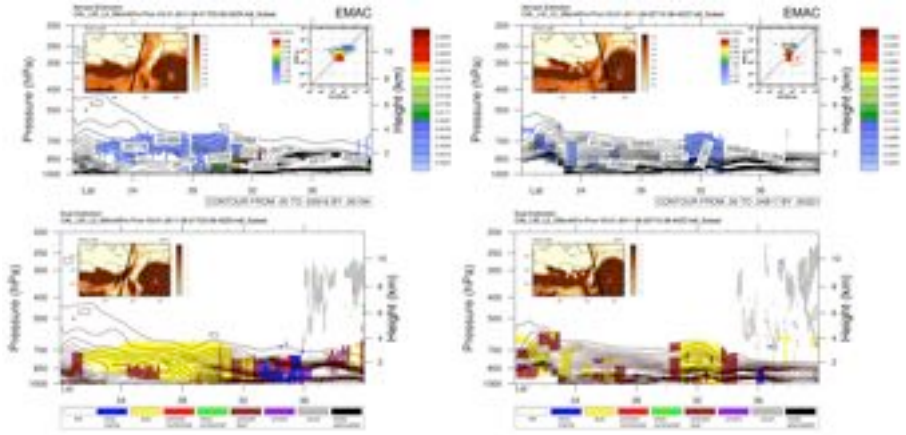

Figure 11. Collocated EMAC calculations and CALIPSO observations of extinction and dust load for two different CALIPSO tracks during the first dust outflow event – overpasses from Africa to the EM, (top) dust extinction (bottom) CALIPSO aerosol classifications, dust extinction (black line) and total extinction (brown dotted line).

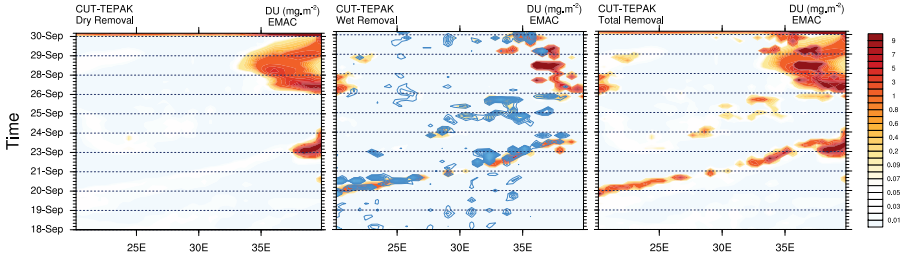

Figure 12. Time evolution of dry, wet and total removal of dust at CUT-TEPAK; (blue) TRIMM observations, (orange) EMAC precipitation (see text).

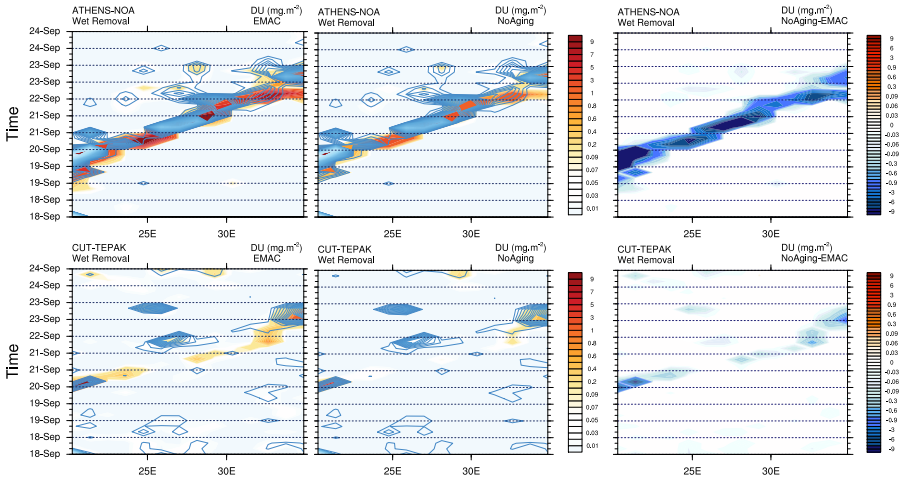

Figure 13. Time evolution of dust wet removal at the CUT-TEPAK and ATHENS-NOA stations for two simulations considering aged dust (EMAC) and non-aged, pristine dust particles (NoAging); (blue) TRIMM observations, (orange) EMAC precipitation (see text).

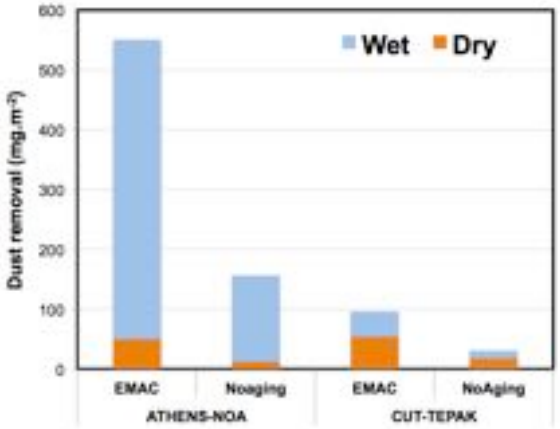

Figure 14. Sensitivity of dust removal (wet and dry) to dust aging: integrated dust removal over the period from 18 to 24 September, 2011.

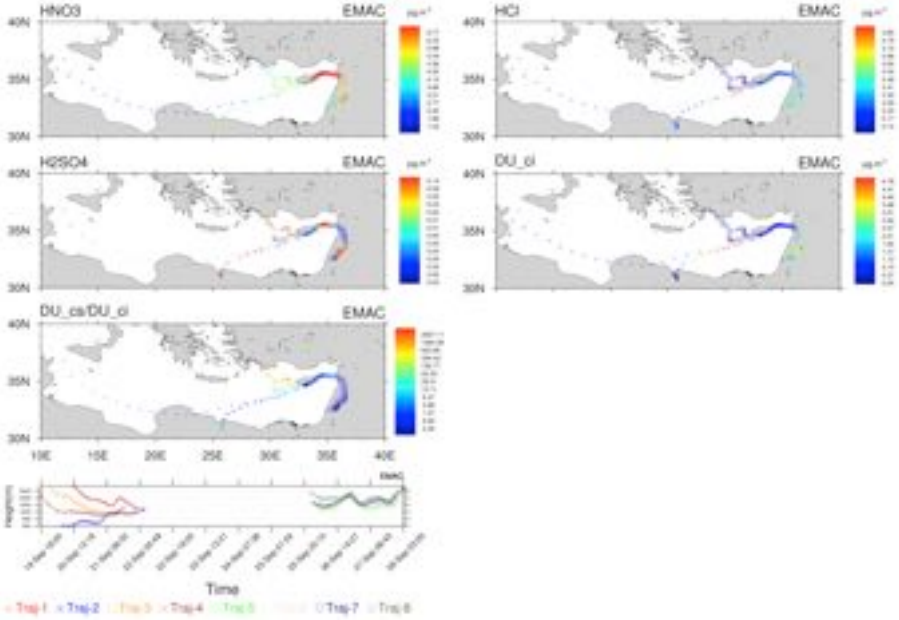

Figure 15. Sampled model concentrations for both dust outflow events; HNO_3, H_2SO_4, HCl, insoluble (pristine) dust fraction (DU_ci) and the aged dust proxy, ADP (DU_cs/DU_ci).

Dust-Air Pollution Dynamics over the Eastern Mediterranean
acp-2015-109
Reply to Anonymous Referee #1

by M. Abdelkader, S. Metzger, R. E. Mamouri,
M. Astitha, L. Barrie, Z. Levin, and J. Lelieveld

June 12, 2015

We thank the anonymous referee for the constructive comments – hopefully addressed satisfactorily with this reply. Modifications of the manuscript are summarized in Table 1. Please also note the modifications in Table 1-5 in our reply to referee #2.

1 AOD

Since the EMAC model distinguishes dust particles (mainly coarse mode) and anthropogenic particles (mainly fine mode), why not showing the AERONET comparisons in more detail? AERONET provides also coarse-mode and fine-mode AOD! Because the focus later on is on CUT-TEPAK comparisons, one could do these specific comparisons at least for the Cyprus AERONET station.

First of all, to clarify the complexity of the EMAC model used in this study and to answer the additional question raised by referee #2, we have modified the model description section to include the following paragraph in the revised MS (see our reply to referee #2):

Our model version distinguishes aerosol particles in 7 modes, 4 Soluble (nucleation, aitken, accumulation, coarse) and three INSoluble modes (aitken, accumulation, coarse) with the complexity of the aerosol thermodynamics as investigated in Metzger et al. (2006), by considering case F4 since ISORROPIA-II used here does not include organic salt compounds in the gas/aerosol partitioning and aerosol neutralization framework. Within EMAC, the dust particles are emitted online following Astitha et al. (2012) (e.g., governed by model dynamics, precipitation and soil moisture) in either the INSoluble accumulation and/or coarse mode and only upon aging and transport they can be transferred to the respective Soluble accumulation and/or coarse modes. The aging depends on the available condensable compounds calculated within the chemistry scheme (Sander et al., 2005). In addition, via coagulation and hygroscopic growth the size-distribution can change and small particles are transferred to larger sizes, i.e., for dust from accumulation to coarse, whereby hygroscopic growth of bulk dust and dust salt compounds is only allowed in the soluble modes. For the latter we explicitly account for the water uptake of various major mineral salt compounds, i.e., $CaSO_4$, $Ca(NO_3)_2$, $CaCl_2$, $MgSO_4$, $Mg(NO_3)_2$, $MgCl_2$, Na_2SO_4, $NaNO_3$, $NaCl$, K_2SO_4, KNO_3, KCl, whereby the mineral cations Mg^{2+}, Na^+ and K^+ are only considered as tracers for the online calculated sea salt emissions, while K^+ is additionally used for biomass burning emissions being emitted here only in the insoluble aitken mode. Thus, the dust particles can be present in our set-up in four modes, each

represented by various calcium compounds that chemically characterize the bulk dust emissions depending on the level of aging. Note that we have limited the dust neutralization reactions in this work to calcium to be able to separate the dust associated water uptake and associated aging from sea salt effects. Since our set-up is flexible, the level of aerosol neutralization complexity can/will be changed for other application tasks. For the current modeling study though, this set-up represents the dust air-pollution dynamics over the Eastern Mediterranean well.

Lumping together a mass and number based size-distribution in one fine and coarse mode can be done, but a comparison with observations of optically derived size-distributions needs to be interpreted with great care. There are many uncertainties on both sides. Therefore we had omitted such a comparison in the manuscript. Nevertheless, to satisfy the referees request, we show the fine and coarse mode AOD for the AERONET observations and the EMAC model results for the CUT-TEPAK station, Cyprus. Figure 1 reveals that the fine mode AOD is dominating the total AOD during September 2011. The model compares well with the AERONET observations, especially during the dust outflow-2 on 28^{th}. AERONET shows an AOD of 0.4 for the coarse mode contribution to the total AOD of 0.6, which is underestimated by EMAC as a result of the steep gradient of the dust load. The dust outflow-2 was predicted to be slightly more east (see discussion of the LIDAR results below).

I know that regional dust transport models have their difficulties with correct dust uptake (emissions) by the atmosphere, and I would like to know what the result is here (EMAC), when using a global model with even coarser resolution than these regional models have.

To satisfy this request, we include a quantitative model comparison of our EMAC results with DREAM (`http://www.bsc.es/earth-sciences/mineral-dust/catalogo-datos-dust`) in this reply. Figure 2 shows the dust load and outflow for the 28^{th} September at noon. Interestingly, both models predict a dust outflow and a dust front which just has touched on Cyprus. These dust-fronts are associated with a very steep gradient of the dust concentrations, which strongly increases a few longitudes to the East. But, compared to the LIDAR observations, both models may not have captured fully the outflow dynamics along the south side of the Troodos mountains, which are up to 2000 meters high and a natural barrier for the dust layer, which peaks around 1500 meters (see discussion of the LIDAR results below). Of course, matching one station on a small island at a given time is an issue that is almost impossible to be accurately resolved by any global model, especially by a climate model (despite sophisticated nudging technique and the relatively high resolution). For this task, higher resolution regional models must be used.

The advantage of regional models clearly is the higher resolution, which can resolve the orography with grid boxes down to a few kilometers, although for atmospheric chemistry applications a resolution of 25-50 km is typical. This advantage cannot be met with a global chemistry-climate model such as EMAC. Even not closely with our high resolution set-up, i.e., T255, which is with a grid box size of $\approx 50\ km$ not only computationally very demanding, but also beyond the state-of-the-art that has been applied for this topic so far. But on the other hand, the advantage of our EMAC version is that dust emissions are calculated online, i.e., fully coupled with meteorology and radiation (being nudged towards observation), without any limitation and assumptions on the moisture, dust and air pollution fluxes at the regional domain boundaries. The latter is also relevant here as the dust is transported over large distances. And this advantage can compensate for the disadvantage of using a lower resolution in case of dust-air pollution dynamics. Ideally, a consistent coupling of equally complex models that represent at least the details currently considered in our study would be required for localized forecasts of individual stations, especially if located around a coast-line of islands with relatively high mountains. Clearly, such applications or a detailed comparison goes far beyond the current work – it remains a challenging subject for follow-up studies.

2 Vertical profiling

Lidar provides the potential to distinguish dust and fine-mode particles, too. There is an EARLINET polarization lidar at Limassol, and I found in AMT a paper (Mamouri et al., 2014) dealing with the same time period as shown here (27-29 September 2011). Why do you not include these observations in this paper in the frame of a thorough comparison? I have long experience with lidar/model comparisons in the case of dust and know that these comparisons usually show large discrepancies between lidar and modeled dust profiles. I assume (speculate) that this is similar here, and I further speculate that this is the reason for ignoring the lidar observations. Nevertheless, progress in science arises from discrepancies! So, please show these comparisons, at least for the published strong dust outbreak (28-29th September).

Although a comparison is not straight forward, mainly because of the assumptions on the treatment of extinction of dust particles at both sides, we have prepared such comparison which will be included in the revised manuscript.

The following section will be included in the revised manuscript:
(with the attached Figure 3 numbered as Figure 10 in the revised MS)

Section 3.3.2 – EMAC versus ground based LIDAR profiles

The vertical structure of the dust outflow-2 is compared to ground based LIght Detection And Ranging (LIDAR) measurements of the Cyprus University of Technology (CUT) in Limassol, Cyprus, which also hosts the AERONET station. The LIDAR observations have been recently used to study dust outflows over the EM, including the dust outflow-2 considered in our study (Mamouri et al., 2013; Nisantzi et al., 2014; Mamouri and Ansmann, 2014, 2015). For a consistent comparison, the LIDAR observations are averaged within the model vertical grid box.

Figure 10 shows the simulated and observed total and dust only extinction at CUT-TEPAK. The model results are shown at three different longitudes: 33 °E at CUT-TEPAK (EMAC), 34°E (EMAC-1) and 35°E (EMAC-2), with all longitudes referring to the latitude of the CUT-TEPAK station (34.675°N). The comparison shows that EMAC captures the LIDAR signal, but 2° (about 200 km) more to the east. This underestimation decreases with each profile further east, indicating a steep gradient of the model dust layer concentration that is associated with the front of the dust-outflow-2 (shown in Fig. 6 and 7). Although the magnitude of the model extinction is predicted lower at the CUT-TEPAK station at both days, EMAC captures the observed peak at 1.5 km height (2nd day) with a 1.8 km dust layer height well, given the relatively coarse vertical grid resolution of the model (which is 500 m at that height).

Interestingly, the calculated vertical extent of the dust layer is wider than the LIDAR signal, which indicates that the total aerosol layer is thicker, at least a few hundred kilometers eastward. This might be related to flow disturbance by the orography, and/or a result of the contribution of other compounds that are considered in our model simulation. The vertically integrated dust extinction is similar to the total extinction profiles for both EAMC and the observations, but the predicted concentration maximum of the dust layer is closer to the observations for the second day. For the first day, EMAC does not capture the observed dust signal, but the total AOD (integral of the area under the profile) is comparable to the AERONET AOD shown in Fig. 4 for both days.

Let me start with Figure 6: The satellite images indicate a lot of dust over Cyprus on 28th September as well as on 29 September. Figure 7: Why did you calculate trajectories for Limassol (22 Sep) and then for the northeastern peak of Cyprus (28th Sep, evening)? Why not again Limassol? This is strange and seems to be arbitrarily selected. In the evening of 28th Sep there was probably dust everywhere over Cyprus according to the images in Figure 6. So, please show the trajectories for Limassol, only!

The objective is to study the dynamics of the dust air-pollution interaction during two dust events. The MODIS satellite image (Figure 6 p. 7526 in the MS) shows dust outflow over the EM, including Cyprus. The model results (Fig. 9 p. 7529 in the MS) resolve the dust outflow over the EM, however, with a strong dust gradient over the eastern part of Cyprus on 28^{th}, September, which is also predicted by the DREAM model (see Fig. 2). On the other hand, the HYSPLIT back trajectories (Fig. 7 pg 7527 of the MS), are based on the NCEP reanalysis data which has a resolution of 270 km. Such coarse resolution seems in this case insufficient as is does not capture the strong gradient associated with the atmospheric dynamics over Cyprus. As a result, the calculated HYSPLIT back trajectories at Limassol (CUT-TEPAK) indicated an air mass that has reached CUT-TEPAK originating from Turkey, instead from the Arabian Desert as indicated by the MODIS image (Figure 6 p. 7526) and our EMAC model results (shown in Fig. 9 p. 7529) and the results of the DREAM model (see Fig. 2). For this reason, we have calculated the back trajectories at the eastern part of Cyprus, where our model dust load is also more consistent with the MODIS image. In order to be consistent with the back trajectories, back trajectories could be calculated using the meteorological field driven by regional and high resolution model for better representation of the topography with an advanced back trajectory model such as FLEXPART. But this is beyond this study.

Figures 8, 9 show very nice model results covering the two outbreak situations. Height- longitude plots of dust distribution are shown. You emphasize the CUT-TEPAK station, so these dust cross sections are for 34.5 North? Right? Please state that clearly! What does "zonal dust" then mean in this context? A dust value at 700 hPa, for 30E and 34.5N describes just one value for the given location, not for a zonal belt?

We apologize for the typo. The figure shows the meridional mean of the dust at CUT-TEPAK location (34.675^{o}N). The figure caption is changed to:

Time series of (top) dust load and (bottom) meridional mean for the first event at CUT-TEPAK location (34.675°N). The green shaded area represents the orography.

Now, a comparison between the Limassol lidar versus EMAC dust profile (dust extinction, overall aerosol extinction profiles) is required. Maybe the best time for comparison is the morning of 29 September (according to the images in Figure 6). I realize from Figure 9 that there are strong horizontal dust inhomogeneities (in the model results), especially close to Limassol, so the lidar comparison may reflect that by strong deviations between observation and modeling. This must be discussed. But at least the geometrical structure (base and top heights of the dust layer) should match, I speculate.

We have addressed this point by the new Section 3.3.2 which will show a comparison of our EMAC results with the suggested LIDAR observations at CUT-TEPAK. The results of this comparison (and the new Section 3.3.2) have been presented above.

Finally, Figure 10: I appreciate very much that CALIPSO data are included in the comparison. This is not just an easy task! CALIPSO provides backscatter coefficients. How did you get the extinction values? What lidar ratios were applied? Probably 40sr for pure dust and 60sr for polluted dust, and 20sr for marine!

As shown in the manuscript (p. 7507 line 10) CALIPSO Level 2 version 3.01, 5 km aerosol profile (APro-Prov) product is used. The lidar ratios used to calculate the extinction of pure dust, polluted dust and marine aerosols are: 40 sr, 65 sr and 20 sr, respectively (Winker et al., 2009). Fig. 4 (below) shows the ratios and size distribution as used in CALIPSO aerosol model.

CALIPSO uses the linear iterative method to derive profiles of volume backscatter and extinction coefficients from both clouds and aerosols. In the CALIPSO extinction analysis, features are analyzed or solved (their particulate backscatter and extinction profiles retrieved) using lidar ratios appropriate to the type of cloud or aerosol layer of which they are composed. As a scene, or any profile for that matter, can contain features of different types. Different lidar ratios are used in different regions of the scene or profile. The lidar ratio is considered to be constant over certain intervals within each backscatter profile, as determined by the layer detection and scene classification algorithms. A unique feature of the CALIPSO lidar analysis is that it attempts to average signals in atmospheric regions where the optical properties are uniform and the signal strengths are comparable (Vaughan et al., 2009). Perhaps the single most difficult task among the scene classification algorithms is determining the appropriate lidar ratio to be used in the optical analyses of aerosol layers as a results of the very high ground speed of the satellite (7 km s^{-1}) compared to the stationary ground based LIDAR. Field measurements of aerosol lidar ratios in the surface-attached aerosol layers (SAL) vary from 15 sr to in excess of 120 sr (Vaughan et al., 2004). Lidar-only measurements of lidar ratios require a Raman lidar or a high spectral resolution lidar (HSRL). CALIPSO therefore determines a value for Sa using a model-matching scheme: the optical, geophysical (e.g., latitude, longitude), and temporal (season) characteristics of the 532 layer are used as decision points to navigate through a flow chart that ultimately selects a most likely aerosol model for each aerosol layer.

And what I know from the Kanitz paper (AMT 2014?) the jumps (in color) in the extinction values are artefacts and due to the jumps in the extinction values when you go from laser foot prints over the Mediterranean Sea (lidar ratio 20) to land surfaces (lidar ratio of 40/60) and back to sea surfaces (20) again. These strong aretfacts should be mentioned.

The comparison between CALIPSO and the EMAC model (upper panel of Fig. 10 p. 7530 in the MS) includes only the CALIPSO pure dust classification. Artifacts of marine aerosol layers that extend over land may indeed produce a mixed signal potentially affecting the CALIPSO classification over land (Fig. 10, lower panel). For our comparison this is less relevant, since we focus on a distinct dust layer over the Mediterranean sea. And the CALIPSO classification is most safe for dust cases. An even more detailed combination of model results, ground-based and satellite observations would be desired to better distinguish between pure dust and polluted dust events. But such consistent data is not available. Nevertheless, our model results can give additional insight in the effects of mixing of dust and air-pollution, and may be used to challenge results such of Kanitz et al. (2014). Again, this is beyond the scope of this study. In this respect, we see our modeling study as one contribution to an overall very challenging effort – both from an observational point of view as well as from our modeling point. We look forward to a closer collaboration which will help improving our understanding of this very important subject.

The following text is added to the revised MS:

In addition, the CALIPSO aerosol type classification could overestimate the extinction and the optical depth for marine aerosols. This may add artifacts to the mixed dust classification over land (Kanitz et al., 2014).

Figure 10: I cannot see (or distinguish) brown and black isolines. . .?

We apologize that brown iso-lines are not distinguishable. Unfortunately, this is a result of the graphic conversion during the typesetting procedure, which converted vector graphics to raster images to reduce the file size. But we will keep the quality of the vector images in the final manuscript, so that the details are also visible without zooming into the image.

References

Astitha, M., Lelieveld, J., Abdel Kader, M., Pozzer, A., and de Meij, A.: Parameterization of dust emissions in the global atmospheric chemistry-climate model EMAC: impact of nudging and soil properties, Atmospheric Chemistry and Physics, 12, 11 057–11 083, doi:10.5194/acp-12-11057-2012, URL http://www.atmos-chem-phys.net/12/11057/2012/, 2012.

Kanitz, T., Ansmann, A., Foth, A., Seifert, P., Wandinger, U., Engelmann, R., Baars, H., Althausen, D., Casiccia, C., and Zamorano, F.: Surface matters: limitations of CALIPSO V3 aerosol typing in coastal regions, Atmospheric Measurement Techniques, 7, 2061–2072, doi:10.5194/amt-7-2061-2014, URL http://www.atmos-meas-tech.net/7/2061/2014/, 2014.

Mamouri, R. E. and Ansmann, A.: Fine and coarse dust separation with polarization lidar, Atmospheric Measurement Techniques, 7, 3717–3735, doi:10.5194/amt-7-3717-2014, URL http://www.atmos-meas-tech.net/7/3717/2014/, 2014.

Mamouri, R. E. and Ansmann, A.: Estimated desert-dust ice nuclei profiles from polarization lidar: methodology and case studies, Atmospheric Chemistry and Physics, 15, 3463–3477, doi:10.5194/acp-15-3463-2015, URL http://www.atmos-chem-phys.net/15/3463/2015/, 2015.

Mamouri, R. E., Ansmann, A., Nisantzi, A., Kokkalis, P., Schwarz, A., and Hadjimitsis, D.: Low Arabian dust extinction-to-backscatter ratio, Geophysical Research Letters, 40, 4762–4766, doi:10.1002/grl.50898, URL http://dx.doi.org/10.1002/grl.50898, 2013.

Metzger, S., Mihalopoulos, N., and Lelieveld, J.: Importance of mineral cations and organics in gas-aerosol partitioning of reactive nitrogen compounds: case study based on MINOS results, Atmospheric Chemistry and Physics, 6, 2549–2567, doi:10.5194/acp-6-2549-2006, URL http://www.atmos-chem-phys.net/6/2549/2006/, 2006.

Nisantzi, A., Mamouri, R. E., Ansmann, A., and Hadjimitsis, D.: Injection of mineral dust into the free troposphere during fire events observed with polarization lidar at Limassol, Cyprus, Atmospheric Chemistry and Physics, 14, 12 155–12 165, doi:10.5194/acp-14-12155-2014, URL http://www.atmos-chem-phys.net/14/12155/2014/, 2014.

Sander, R., Kerkweg, A., Jckel, P., and Lelieveld, J.: Technical note: The new comprehensive atmospheric chemistry module MECCA, Atmospheric Chemistry and Physics, 5, 445–450, doi:10.5194/acp-5-445-2005, URL http://www.atmos-chem-phys.net/5/445/2005/, 2005.

Vaughan, M. A., Young, S. A., Winker, D. M., Powell, K. A., Omar, A. H., Liu, Z., Hu, Y., and Hostetler, C. A.: Fully automated analysis of space-based lidar data: an overview of the CALIPSO retrieval algorithms and data products, pp. 16–30, doi:10.1117/12.572024, URL http://proceedings.spiedigitallibrary.org/proceeding.aspx?articleid=851227, 2004.

Vaughan, M. A., Powell, K. A., Winker, D. M., Hostetler, C. A., Kuehn, R. E., Hunt, W. H., Getzewich, B. J., Young, S. A., Liu, Z., and McGill, M. J.: Fully Automated Detection of Cloud and Aerosol Layers in the CALIPSO Lidar Measurements, Journal of Atmospheric and Oceanic Technology, 26, 2034–2050, doi:10.1175/2009JTECHA1228.1, URL http://journals.ametsoc.org/doi/abs/10.1175/2009JTECHA1228.1, 2009.

Winker, D. M., Vaughan, M. A., Omar, A., Hu, Y., Powell, K. A., Liu, Z., Hunt, W. H., and Young, S. A.: Overview of the CALIPSO Mission and CALIOP Data Processing Algorithms, Journal of Atmospheric and Oceanic Technology, 26, 2310–2323, doi:10.1175/2009JTECHA1281.1, URL http://journals.ametsoc.org/doi/abs/10.1175/2009JTECHA1281.1, 2009.

Table 1: Revised manuscript – Modifications for referee#1. Please also note the modifications in Table 1-5 in our reply to referee #2.

no.	P. no.	Line no.	Before	Correction
1	7493	Authors	M. Abdelkader, S. Metzger, M. Astitha, Z. Levin, and J. Lelieveld	M. Abdelkader, S. Metzger, R. E. Mamouri, M. Astitha, L. Barrie, Z. Levin, and J. Lelieveld
2	7507	8		New Section 3.3.2 (and adjusted labeling of the following sections)
3	7507	20	Added text before "Therefore, the CALIPSO data .....":	In addition, the CALIPSO aerosol type classification could overestimate the extinction and the optical depth for marine aerosols. This may add artifacts to the mixed dust classification over land (Kanitz et al., 2014).
4	7514	16	Added text to acknowledgment:	The authors thank the Remote sensing and Geo-Environment Research laboratory of Cyprus University of Technology (CUT) for providing the LIDAR extinction profiles at the CUT-TEPAK station.
5	7528-9	caption	Time series of (top) dust load and (bottom) vertical cross-sections at the CUT-TEPAK station for the first event, the green shaded area represents the orography.	Time series of (top) dust load and (bottom) meridional mean for the first event at CUT-TEPAK location (34.675°N). The green shaded area represents the orography.
6	–	–	Added Fig. 3 of this reply	In the MS, labeled Figure 10 (adjusted labeling of figures).
7	–	–	No Supplement.	Figure 1 will be included in a Supplement.

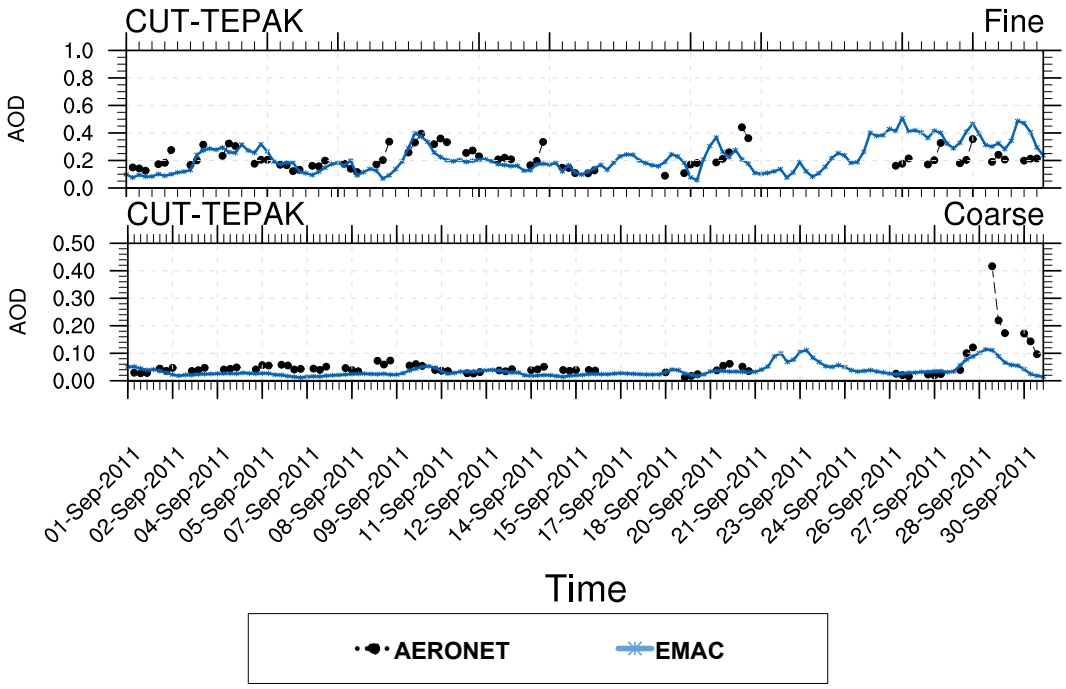

Figure 1: Aerosol fine mode (top) and coarse mode (bottom) AOD: EMAC model (blue lines) versus AERONET station observations (black lines). This figure is added to the supplement.

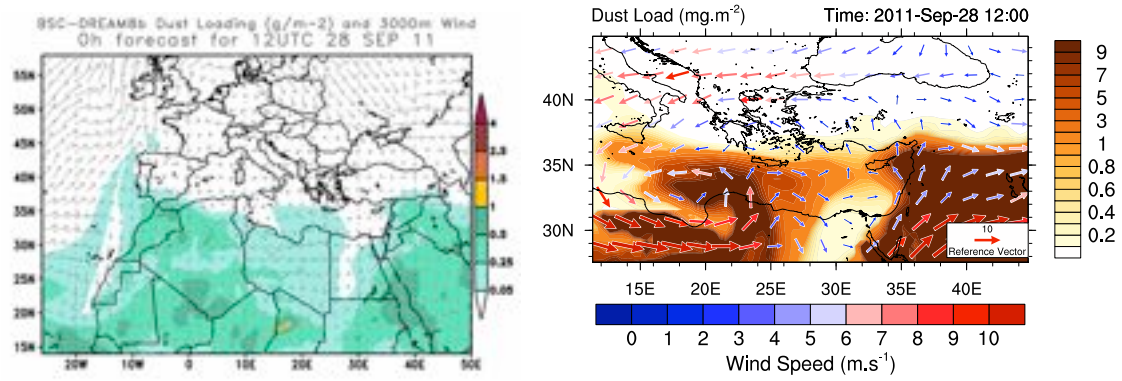

Figure 2: Dust load on 28^{th} September 2011 for DREAM (left) and EMAC model (right).

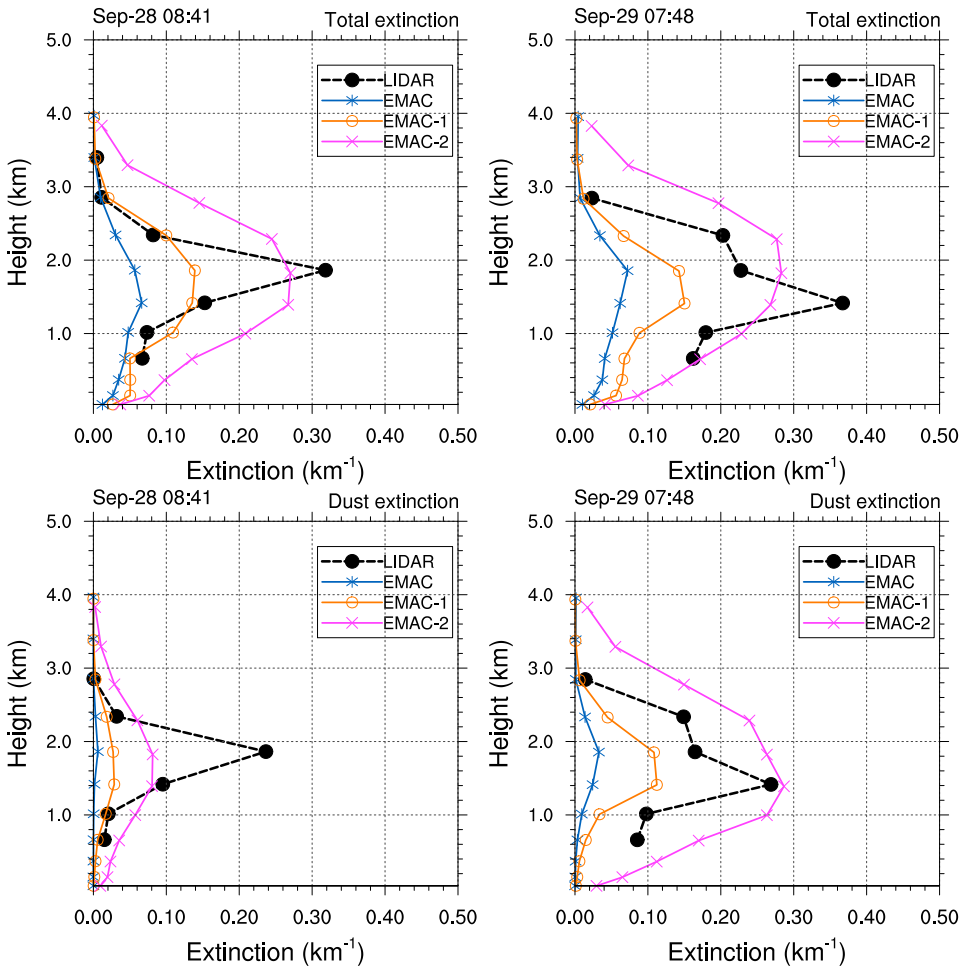

Figure 3: Comparison between the modeled and the observed total and dust only extinction at CUT-TEPAK station at different longitudes: 33 °E (EMAC) at CUT-TEPAK station, 34°E (EMAC-1) and 35°E (EMAC-2); all longitudes refer to the latitude of CUT-TEPAK (34.675°N). This figure is included in the revised MS.

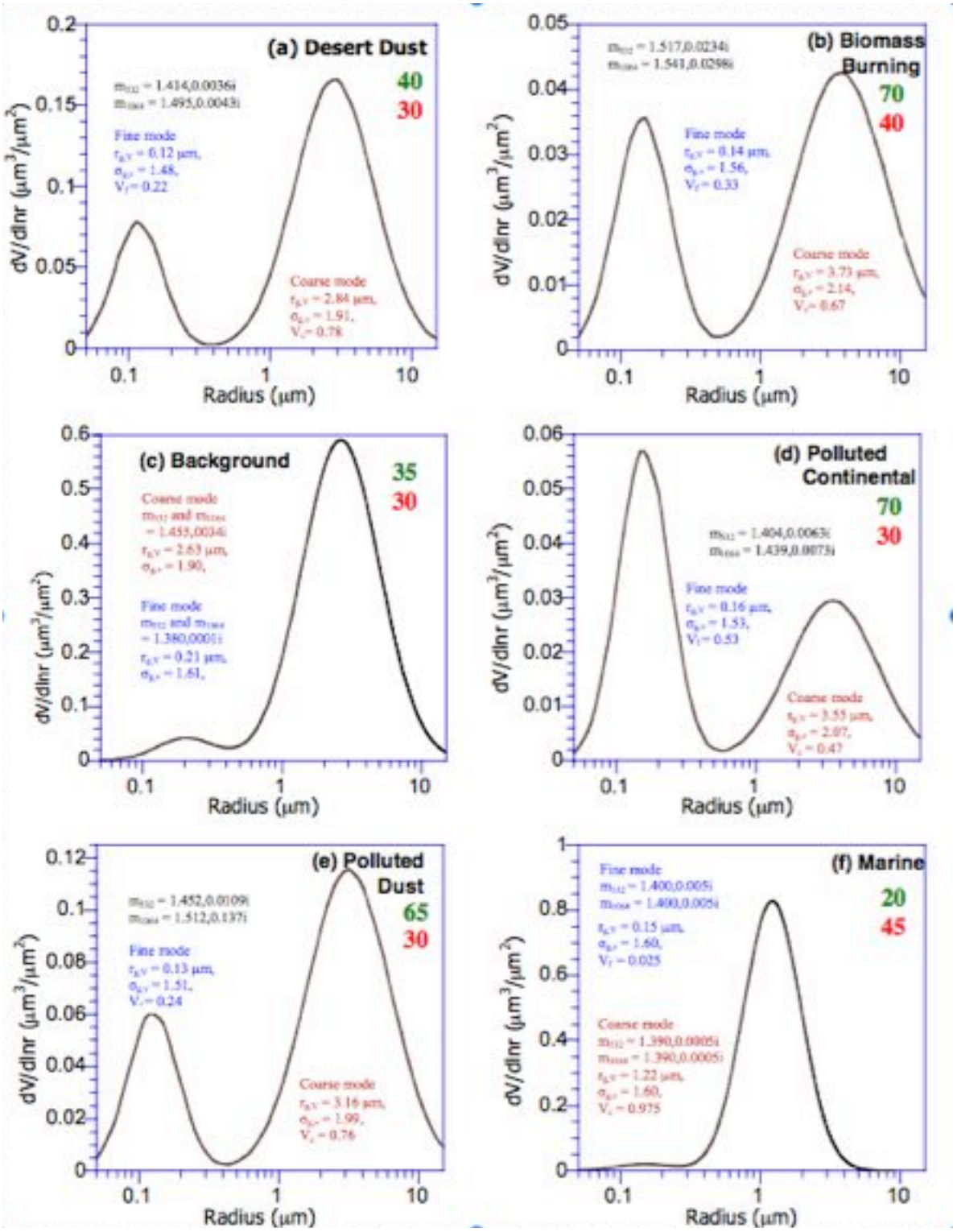

Figure 4: The size distribution and microphysical properties of the CALIPSO aerosol models. For each model, extinction/backscatter ratio S_a at 532nm (green) and 1064 nm (red) are shown.

Dust-Air Pollution Dynamics over the Eastern Mediterranean
acp-2015-109
Reply to Anonymous Referee #2

by M. Abdelkader, S. Metzger, R. E. Mamouri,
M. Astitha, L. Barrie, Z. Levin, and J. Lelieveld

June 12, 2015

We thank the anonymous referee for the constructive comments – hopefully addressed satisfactorily with this reply. Modifications of the manuscript are summarized in Table 1-5. Please also note the modifications in Table 1 in our reply to referee #1.

The manuscript attempts to pin down the importance of the chemical aging process of dust over the Eastern Mediterranean. Aging occurs when polluted air laden with acids (for ex: H2SO4, HNO3, HCl...) encounters parcels containing dust. This is a well chosen topic relevant to ACP, but the way the authors treat the results significance does not establish the proof that aging is the main cause for the observed decrease in dust lifetime and loading. To convince the reader with the results from model, the authors would have to show that it mimics the atmosphere behavior. That includes two points that I could not find in the paper:

1. Show that a majority from the air mass that encounters air pollution are aged. A number of factors relevant to this aging being omitted from the discussion (see below)

The EM is subject to intercontinental transport of air pollution from Europe, North America and Asia, which increases the loadings of aerosols and precursor gases during the usually dry summer period and the lack of sufficient precipitation. Especially the loading of acids such as H_2SO_4 and HNO_3 are enhanced, as a result of the high insulation and the resulting photo-oxidation of the ubiquitous gaseous air pollutants (e.g., NO_x and SO_2 of ship and road traffic and waste and biomass burning). This is confirmed by numerous EMAC modeling studies and observations (Lelieveld et al., 2002; Metzger et al., 2006; Joeckel et al., 2010; de Meij and Lelieveld, 2011; de Meij et al., 2012; Pozzer et al., 2012; Lyamani et al., 2015, among others). The current study is based on the EDGARv4 emissions set (Pozzer et al., 2012) which has been prepared in the framework of the CIRCE project with a focus on the Mediterranean region as shown in p. 7498 line 25 in the MS. All EMAC studies show a high aerosol loading over the EM that is needed for dust-air pollution interaction. To demonstrate this, Figure 1 will be added to the supplement of the revised MS. The upper panel shows an indicative air pollution loading, the lower panel the corresponding cross section passing through CUT-TEPAK station. The air pollution loading represents the vertical integral (burden) of the mass concentration $[mg\ m^{-2}]$ of (left) total inorganic acids ($HCl+HNO_3+H_2SO_4$) that are present in the gas phase, maintaining gas-aerosol equilibrium, (right) the corresponding lumped aerosol burden ($SO_4^{2-}+HSO_4^-+NO_3^-+NH_4^+$+$H_2SO_4$); both average over 20^{th} September - 1^{st} October 2011.

The pollution loading basically covers the northern part of the EM and decreases eastwards. Figure 1 is consistent with the back trajectories (Fig. 14) shown in the MS, which support the north-southeast air pollution gradient that seems to be typical for the Mediterranean basin.

2. That the hygroscopicity of the dust exposed to acids is well represented.

First of all, to clarify the complexity of the EMAC model used in this study and to answer the additional question raised by referee #1, we will modify the MS to include the following paragraph in the model description section (details are shown in the table of modifications):

Our model version distinguishes aerosol particles in 7 modes, 4 Soluble (nucleation, aitken, accumulation, coarse) and three INSoluble modes (aitken, accumulation, coarse) with the complexity of the aerosol thermodynamics as investigated in Metzger et al. (2006), by considering case F4 since ISORROPIA-II used here does not include organic salt compounds in the gas/aerosol partitioning and aerosol neutralization framework. Within EMAC, the dust particles are emitted online following Astitha et al. (2012) (e.g., governed by model dynamics, precipitation and soil moisture) in either the INSoluble accumulation and/or coarse mode and only upon aging and transport they can be transferred to the respective Soluble accumulation and/or coarse modes. The aging depends on the available condensable compounds calculated within the chemistry scheme (Sander et al., 2005). In addition, via coagulation and hygroscopic growth the size-distribution can change and small particles are transferred to larger sizes, i.e., for dust from accumulation to coarse, whereby hygroscopic growth of bulk dust and dust salt compounds is only allowed in the soluble modes. For the latter we explicitly account for the water uptake of various major mineral salt compounds, i.e., $CaSO_4$, $Ca(NO_3)_2$, $CaCl_2$, $MgSO_4$, $Mg(NO_3)_2$, $MgCl_2$, Na_2SO_4, $NaNO_3$, $NaCl$, K_2SO_4, KNO_3, KCl, whereby the mineral cations Mg^{2+}, Na^+ and K^+ are only considered as tracers for the online calculated sea salt emissions, while K^+ is additionally used for biomass burning emissions being emitted here only in the insoluble aitken mode. Thus, the dust particles can be present in our set-up in four modes, each represented by various calcium compounds that chemically characterize the bulk dust emissions depending on the level of aging. Note that we have limited the dust neutralization reactions in this work to calcium to be able to separate the dust associated water uptake and associated aging from sea salt effects. Since our set-up is flexible, the level of aerosol neutralization complexity can/will be changed for other application tasks. For the current modeling study though, this set-up represents the dust air-pollution dynamics over the Eastern Mediterranean well.

Note that the water uptake of aged dust particles is based in this study on ISORROPIA-II and on the full gas-liquid-solid partitioning following (Metzger et al., 2006). Since ISORROPIA-II is widely used in atmospheric air pollution modeling, we can assume that the hygroscopicity and associated water uptake of dust particles exposed to acids is represented well. Furthermore, there are not many studies which explicitly resolve the thermodynamics of such a complex system of aerosol and precursor gases, thermodynamics and aerosol dynamics. This study considers calcium as dust tracer and $HCl, HNO_3, and H_2SO_4$ for acidic uptake by calcium. The calcium salt compounds, $CaSO_4$, $Ca(NO_3)_2$, $CaCl_2$, are subject to water uptake, however, the $CaSO_4$ is negligible, due to the relative high deliquescence humidity which is close to unity.

To clarify the treatment of the dynamical uptake of gases on dust aerosols in our EMAC study, we add the following paragraph being part of the model description section:

Within GMXe, the aging of dust aerosols depends on the total particle surface area and on the concentrations of the aerosol precursor gases (Pringle et al., 2010). The uptake of gases is

kinetically limited considering random motion and diffusion processes that govern the condensation. The rate constant for the condensation on dust particles is given by Eq. 1

$$D_{flux} = \frac{4\pi D_f^2 r_w}{\frac{4D_f}{\nu r_w a_i} + \frac{r_w}{r_w + z_{f1}}} \quad (1)$$

where r_w is the ambient (wet) radius, D_f the temperature dependent diffusion coefficient defined by $D_f = 0.073\ P \left(\frac{T}{T_{ref}}\right)^{\frac{3}{2}}$, P the pressure, T the temperature and T_{ref} the reference temperature (298.15 K). ν denotes the particle mean velocity, defined by $\sqrt{\frac{8R_gT}{\pi M_g}}$, with R the gas constant ($8.31 J\ mol^{-1}K^{-1}$), M_g the molar mass, z_{f1} the mean free path length of the kinetic regime, and a_i the accommodation coefficient (Fuchs and Davies, 1989; Seinfeld and Pandis, 2006). In the current setup we use the accommodation coefficients 0.1, 0.01, 0.01 for sulfuric, hydrochloric and nitric acid, respectively. These values have been empirically determined by a comprehensive modeling analysis, which will be presented separately. The uptake of acids is calculated for each particles size, i.e., for dust for the insoluble accumulation and coarse mode.

Both points require a careful comparison with observations from either or both laboratory and field studies. Even when dust is exposed for a long duration to H2SO4 in the laboratory, it hardly becomes hygroscopic. I did not see a review of the work that has been done on this topic. Studies such as the one of Tobo et al. (2009) indicate that in the presence of H_2SO_4, dust gets hardly hydrated except if chloride is present. Another important limiting factor in the uptake of acids and hence in the aging of dust is its calcite content. Fairlie et al. (2010) have treated this limitation but no discussion is made of how this is considered in the present work. Since these factors are paramount to the effect studied here, much more effort should be put to assess whether the model is considering them adequately and this is missing from this work.

This is a good point and the reason why we have explicitly considered the chemical speciation of mineral dust. Our treatment of using the calcium ion to determine the level of bulk dust neutralization through the reaction with inorganic acids such as H_2SO_4, HNO_3, and HCl reflects indeed the situation mentioned. In contrast to $Ca(NO_3)_2$ and $CaCl_2$, $CaSO_4$ does not contribute to water uptake, if the RH is below 99%. The reason is that the relative humidity of deliquescence (RHD) of calcium sulfate is close to unity by room temperature, while the RHD of calcium nitrate and calcium chloride is with ≈ 0.5 and 0.28, respectively, significantly lower. This is the actual reason for the fact that dust particles basically only become hygroscopic once exposed to nitric or hydrochloric acid. Especially, the coating by chlorides leads to hygroscopic growth and associated water uptake at almost all atmospheric conditions, particularly when dust plumes expand over oceans, such at the dust outflow over the EM considered in this study. With the additional model description we address this issue more clearly in the revised MS.

This being said the region of study and the cases chosen are very good choices to address the aging of dust. There is an inference in this work that I did not see well documented. The authors are convinced that in polluted air masses dust grows hygroscopically very rapidly compared to an airmass with dust in the absence of pollution. The simple observations of changes in altitude of the dust layer cannot suffice to prove it. Other factors such as dynamical or thermodynamical can bring the dust layers to a lower altitude, so why claim that this is caused by aerosol growth?

As outlined above, dust particles coated by inorganic acids such as HNO_3 and HCl, or other soluble compounds, can absorb water vapor, which basically depends on the relative humidity (available water mass) and the total mass loading of the coated (aged) dust. The

water uptake is more-or-less proportional to the mass loadings in most cases. In case of sufficient water vapor, the dust particles size increases with humidity until the dust particles either become activated as cloud droplets and potentially washed out by precipitation, or until the water evaporates again as a result of decreased ambient humidity (e.g., transport effects). All processes are considered here in sufficient detail. The aerosol dynamical processes are considered in the GMXe aerosol submodel (Pringle et al., 2010), the aerosol thermodynamics (dust neutralization and water uptake) by the thermodynamic gas-lqiuid-solid equilibrium partitioning module ISORROPIA II (Fountoukis and Nenes, 2007), and for the in- and below cloud scavenging we follow Tost et al. (2006). Note that thermodynamic equilibrium is considered here only for the gas-liquid-solid partitioning, but the uptake of gases on the aerosols is kinetically limited (see above). Additionally, only a small, size-dependent fraction of the bulk dust is used to chemically specify dust reaction in terms of calcium (see below). Both constraints significantly limit the equilibrium water uptake of bulk aerosols, but are somewhat empirical. The dry deposition is described in (Kerkweg et al., 2006) and explicitly depends on the ambient particle size, so that changes in particle radius, e.g., due to dust aging and associated water uptake directly increases the dry deposition.

However, due to lack of observations, we cannot absolutely quantify the effect of dust aging. Nevertheless, our sensitivity study can give an indication and estimates of the consequences of dust–air pollution interactions. Note that our sensitive study (labeled Noaging) does not consider any dust–air pollution interaction (i.e, the condensation of acids on the dust particle surface is not allowed). Both simulations are based on the same meteorological conditions and on exactly the same model set-up (except dust aging). The result of the "Noaging" case is that dust particles remain in the insoluble mode, where hygroscopic growth is generally omitted. This affects particle size, and therefore dry deposition, wet scavenging and the direct radiative forcing of dust particles. Note that the results of our sensitivity are summarized by Figs. 12 and 13 (of the MS). Interestingly, in all our (EMAC) simulations (not all are shown) the deposition has significantly increased in case of dust aging, which basically is a result of the particle hygroscopic growth, coagulation and the condensation of acids. Significant changes of the height of the dust layer is not predicted by the model. There might be an effect of the aged dust particles on the average transport height which might not be resolved by our model, since the model meteorology is nudged towards observations (ECWMF reanalysis) – which however includes air pollution. We may speculate that a pristine atmosphere without or with considerable less air pollution, dust transport might occur at a different (higher?) altitude. But to investigate this, a free running climate model with the same complexity as used here would be required for quantification. This is an interesting subject for a follow-up study but beyond the scope of this work.

The word "rapidly" (p 7513 line 25) is removed since indeed, it cannot be accurately determined so the wording of rapid aging is not really justified.

In the abstract, the sentence: Our results show the importance of chemical aging and deposition of the dust during transport. Needs to be completed by saying for what aspect of dust is this chemical aging important.

The sentence is changed to:

Our results show the importance of chemical aging of dust, which increases particles size, dust deposition and scavenging efficiency during transport, overall reducing the life-time relative to non-aged dust particles.

The following sentence p 7496, lines 11 to 13: "Since Cyprus lows are often associated with precipitation, the residence time of dust particles in the atmosphere can be relatively short (approximately one day).", is vague and the estimation of the residence time is not substantiated.

This comment refers to the dust outflow into the EM based on satellite observations during autumn (Dayan et al., 1991), which indicated a residence time of dust by one day. Since the meteorological condition and level of air pollution that govern this study may not be identical, the residence time may also be different. To clarify, the sentence is modified to:

Since Cyprus lows are often associated with precipitation, the residence time of dust particles in the atmosphere can be relatively short. In case of a barometric trough penetrating from the Red Sea into the EM, it can be as short as one day (Dayan et al., 1991).

Page 7496 lines 24-28 : Especially the interaction between dust and anthropogenic pollution from eastern and western Europe (Levin et al., 2005) in addition to intercontinental air pollution transports from North America and Asia (Lelieveld et al., 2002) deserves attention, being the focus of this study., needs to be reworked

The sentence is changed to:

Especially the interaction of atmospheric dust particles with air pollution from eastern and western Europe and long-range transport from North America and Asia (Lelieveld et al., 2002; Levin et al., 2005, among others) remains to be scrutinized – the focus of this study.

Page 7497, lines 19 to 20 : the fraction of water on dust is very much debated, some authors argue that dust can seldomly uptake dust. You need to review the experimental and field evidence to backup this claim: "The latter includes in- and below cloud scavenging, and depends on the chemical composition of the dust surface, which can include a large fraction of water".

Assuming the referee means "dust can seldomly uptake water", we agree that "can include a large fraction of water" needs to be put in context. We believe that we have clarified this aspect with our above explanations and additional description that will be part of the MS.

To be more precise, the sentence is changed to:

..., which can include a large fraction of water in case dust particles are coated by hydrochloric or nitric acids and/or are exposed to high relative humidity.

Note, although dust particles are insoluble there is a soluble fraction which depends on the dust mineralogy. Calcium rich particles preferentially form calcium sulfate, when coated with sulfuric acid. But this compound is insoluble (as mentioned above) and therefore does not contribute to water uptake, if the relative humidity is below 99%. In contrast, uptake of hydrochloric acids on mineral dust can yield calcium chloride, which can absorb water at RH 28% and therefore increases the hygroscopicity of dust particles (Tobo et al., 2009). But for both cases, the water uptake strongly depends on the available water vapor. For instance, Levin et al. (1996) performed a field study over the EM, showing that dust particles of 20 μm diameter coated with sulfate can grow up to 40 μm under supersaturated conditions as a result of heterogeneous reactions within clouds.
On the other hand, Osada (2013) showed no hygroscopic growth of dust particles in case of sub-saturated conditions. The study of Twohy et al. (2009) further showed dust particle hygroscopicity over the eastern Atlantic ocean only. Mixtures of dust and sea salt particles may contribute to the particle hygroscopicity, depending on the air pollution levels which affects

both the sea salt and mineral dust composition – effects that are explicitly considered in our model study (implicitly by the complexity of the model set-up).
Of course, the hygroscopicity of the dust particle depends on many factors, including morphology, particle size, concentration of acids such as sulfuric, nitric or hydrochloric acid. All of them are difficult to measure and therefore only indirectly accessible. Therefore, we have performed a sensitivity study and compared the model results to multi-platform observations that more-or-less accurately resolve the dynamics of the dust-air pollution interactions. Despite the underlying uncertainties, our model results are at least consistent with different observations.

Page 7500, lines 7 to 11 : We consider the calcium cation (Ca2+) as a chemically reactive tracer on the dust, being emitted in the insoluble accumulation and insoluble coarse modes as a fraction of the dust emission flux (25 and 5% for the accumulation and coarse mode, 10 respectively). These are critical numbers for this paper, the 25% in the accumulation mode is a very large number compared to the composition of dust observed, how was it chosen ? What are the measurements to back it up ?

Calcium is used here only as a proxy for the overall chemical reactivity of the dust particles, which are otherwise (usually) only treated as bulk particles (without any reactivity). The fractions of 25% and 5% have been chosen to represent a different reactivity of fine and coarse mode dust particles, assuming that smaller particles contain eventually a higher amount of soluble ions (implicitly assuming differences in the size-dependent reactivity). Both numbers have been empirically derived from a comprehensive sensitivity study to match the calcium concentrations with observations, with the constraint that at the same time the best comparison with other aerosol species (ammonium, sodium, nitrate, sulfate, chloride, etc) as well as PM and AOD is achieved with respect to various (independent) observations (that include EMEP, CASTNET and AERONET, various satellite and LIDAR data). Part of our analysis is shown by Figure 3, 4, 10-12, of the MS. However, the comprehensive model evaluation will be presented separately. Of course, these numbers depend on the overall model set-up and might be subject to change for a different model complexity.

Page 7508 lines 13 to 16: For this case, both the model and the CALIPSO results show that dust was removed during transport from the atmosphere by wet and dry deposition, since the height of the dust plume decreases from about 4000m over the central Mediterranean on 21 September to about 2000m over the EM on 22 September.. How do you infer directly from a change in height of a dust plume that deposition has occurred?

Our conclusion is based on the dust outflow dynamics (Fig. 8, MS p. 7528) and on the deposition fluxes (Fig. 11, p. 7531), which show that the dust loading has significantly reduced after the frontal system has passed, while the dust deposition has increased during the presence of the frontal system (20 September to 24 September).

The sentence on p.7508, lines 13 to 16, is changed to:

For both cases, the model and CALISPO results show that the dust concentration decreased during the transport and the height of the dust plume decreased from about 4000m over the central Mediterranean on 21 September to about 2000m over the EM on 22 September. The model results showed that the dust loading has significantly reduced after the frontal system has passed (Fig. 8) which enhanced the dust deposition (see next section).

Figure 12 is a consequence of the properties you imposed to aged dust in the model. What evidence do you have that for an air parcel with the same characteristics the size distribution is profoundly changed between a parcel that encounters pollution and one that does not?

The only way to disentangle this question is a model study that represents two identical cases, which only differ with respect to the treatment of aging. This is what has been presented here. With the additional explanation given in this reply, and in the reply to referee #1, we believe to have clarified this point. Again, briefly, there would not be identical size-distributions. The level of aging determines the water uptake, which in turn determines the particle size. Strictly spoken, identical size distributions would yield identical results, since all model feedbacks considered (dry and wet deposition and radiation) are sensitive only to the particle size, but our particle size critically depends on the chemistry, which in turn depends on the dust-air pollution dynamics over the Eastern Mediterranean.

You state page 7512 line 26 that aged dust proxy increases from 1 to 13. What measurements or other evidence back up this number?

This aged dust proxy (ADP) is specific to our model set-up. The number represents (for a particular mode) a ratio of soluble to insoluble dust concentration. A high value indicates a high level of dust aging, since all dust is initially emitted in the insoluble modes and in our EMAC set-up only transferred upon aging to the respective soluble modes. Thus, high ADP value requires a high level of air pollution that suffices to coat the primary dust particles. But more important than the absolute ADP value is its relative change, which nicely reflects the interaction of dust–air pollution dynamics. Unfortunately there are no measurements to compare with. Maybe our results could motivate further studies in this direction.

Page 7513, line 25: you mention that dust is rapidly aged, please give a time it takes for the model in hours/days to age dust with respect to the concentration(s) of acid(s) present and indicate what observations it can be compared to

The only time estimate we can give is that shown in the lower panel of Fig. 14 (p. 7534 of the MS). For instance, for the dust outflow-2, where the dust from Arabian desert enters the Mediterranean basin, the ADP changes from below 1 to more that 6 in less than 5 hours (model output frequency). This is expressed by the sharp change in the trajectory color from dark blue to cyan, indicating that the concentration of the soluble dust must have increased by a factor of 6 in less than 5 hrs. But this number depends on the atmospheric dynamics and cannot be generalized. The word "rapidly" (p 7513 line 25) is removed since indeed, it cannot be accurately determined so the wording of rapid aging is not really justified (see above).

References

Astitha, M., Lelieveld, J., Abdel Kader, M., Pozzer, A., and de Meij, A.: Parameterization of dust emissions in the global atmospheric chemistry-climate model EMAC: impact of nudging and soil properties, Atmospheric Chemistry and Physics, 12, 11 057–11 083, doi:10.5194/acp-12-11057-2012, URL http://www.atmos-chem-phys.net/12/11057/2012/, 2012.

Dayan, U., Heffter, J., Miller, J., and Gutman, G.: Dust Intrusion Events into the Mediterranean Basin, Journal of Applied Meteorology, 30, 1185–1199, doi:10.1175/1520-0450(1991)030⟨1185:DIEITM⟩2.0.CO;2, 1991.

de Meij, A. and Lelieveld, J.: Evaluating aerosol optical properties observed by ground-based and satellite remote sensing over the Mediterranean and the Middle East in 2006, Atmospheric Research, 99, 415–433, doi:10.1016/j.atmosres.2010.11.005, URL http://linkinghub.elsevier.com/retrieve/pii/S016980951000308X, 2011.

de Meij, A., Pozzer, A., Pringle, K., Tost, H., and Lelieveld, J.: EMAC model evaluation and analysis of atmospheric aerosol properties and distribution with a focus on the Mediterranean region, Atmospheric Research, 114-115, 38–69, doi:10.1016/j.atmosres.2012.05.014, URL http://linkinghub.elsevier.com/retrieve/pii/S0169809512001536, 2012.

Fountoukis, C. and Nenes, A.: ISORROPIA II: a computationally efficient thermodynamic equilibrium model for $K^+-Ca^{2+}-Mg^{2+}-NH_4^+-Na^+-SO_4^{2-}-NO_3^--Cl^--H_2O$ aerosols, Atmospheric Chemistry and Physics, 7, 4639–4659, doi:10.5194/acp-7-4639-2007, URL http://www.atmos-chem-phys.net/7/4639/2007/, 2007.

Fuchs, N. A. and Davies, C. N.: The mechanics of aerosols, Dover Publications, New York, 1989.

Joeckel, P., Kerkweg, A., Pozzer, A., Sander, R., Tost, H., Riede, H., Baumgaertner, A., Gromov, S., and Kern, B.: Development cycle 2 of the Modular Earth Submodel System (MESSy2), Geoscientific Model Development, 3, 717–752, doi:10.5194/gmd-3-717-2010, URL http://www.geosci-model-dev.net/3/717/2010/gmd-3-717-2010.html, 2010.

Kerkweg, A., Buchholz, J., Ganzeveld, L., Pozzer, A., Tost, H., and Jckel, P.: Technical Note: An implementation of the dry removal processes DRY DEPosition and SEDImentation in the Modular Earth Submodel System (MESSy), Atmos. Chem. Phys., 6, 4617–4632, doi:10.5194/acp-6-4617-2006, URL http://www.atmos-chem-phys.net/6/4617/2006/, 2006.

Lelieveld, J., Berresheim, H., Borrmann, S., Crutzen, P. J., Dentener, F. J., Fischer, H., Feichter, J., Flatau, P. J., Heland, J., Holzinger, R., Korrmann, R., Lawrence, M. G., Levin, Z., Markowicz, K. M., Mihalopoulos, N., Minikin, A., Ramanathan, V., de Reus, M., Roelofs, G. J., Scheeren, H. A., Sciare, J., Schlager, H., Schultz, M., Siegmund, P., Steil, B., Stephanou, E. G., Stier, P., Traub, M., Warneke, C., Williams, J., and Ziereis, H.: Global Air Pollution Crossroads over the Mediterranean, Science, 298, 794–799, doi:10.1126/science.1075457, URL http://www.sciencemag.org/content/298/5594/794.abstract, 2002.

Levin, Z., Ganor, E., and Gladstein, V.: The Effects of Desert Particles Coated with Sulfate on Rain Formation in the Eastern Mediterranean, Journal of Applied Meteorology, 35, 1511–1523, doi:10.1175/1520-0450(1996)035⟨1511:TEODPC⟩2.0.CO;2, 1996.

Levin, Z., Teller, A., Ganor, E., and Yin, Y.: On the interactions of mineral dust, sea-salt particles, and clouds: A measurement and modeling study from the Mediterranean Israeli

Dust Experiment campaign, Journal of Geophysical Research: Atmospheres, 110, D20 202, doi:10.1029/2005JD005810, URL http://dx.doi.org/10.1029/2005JD005810, 2005.

Lyamani, H., Valenzuela, A., Perez-Ramirez, D., Toledano, C., Granados-Muoz, M. J., Olmo, F. J., and Alados-Arboledas, L.: Aerosol properties over the western Mediterranean basin: temporal and spatial variability, Atmos. Chem. Phys., 15, 2473–2486, doi:10.5194/acp-15-2473-2015, URL http://www.atmos-chem-phys.net/15/2473/2015/, 2015.

Mamouri, R. E., Ansmann, A., Nisantzi, A., Kokkalis, P., Schwarz, A., and Hadjimitsis, D.: Low Arabian dust extinction-to-backscatter ratio, Geophysical Research Letters, 40, 4762–4766, doi:10.1002/grl.50898, URL http://dx.doi.org/10.1002/grl.50898, 2013.

Metzger, S., Mihalopoulos, N., and Lelieveld, J.: Importance of mineral cations and organics in gas-aerosol partitioning of reactive nitrogen compounds: case study based on MINOS results, Atmospheric Chemistry and Physics, 6, 2549–2567, doi:10.5194/acp-6-2549-2006, URL http://www.atmos-chem-phys.net/6/2549/2006/, 2006.

Osada, K.: Water soluble fraction of Asian dust particles, Atmospheric Research, doi:10.1016/j.atmosres.2013.01.001, URL http://linkinghub.elsevier.com/retrieve/pii/S0169809513000124, 2013.

Pozzer, A., de Meij, A., Pringle, K. J., Tost, H., Doering, U. M., van Aardenne, J., and Lelieveld, J.: Distributions and regional budgets of aerosols and their precursors simulated with the EMAC chemistry-climate model, Atmospheric Chemistry and Physics, 12, 961–987, doi:10.5194/acp-12-961-2012, URL http://www.atmos-chem-phys.net/12/961/2012/, 2012.

Pringle, K. J., Tost, H., Metzger, S., Steil, B., Giannadaki, D., Nenes, A., Fountoukis, C., Stier, P., Vignati, E., and Lelieveld, J.: Description and evaluation of GMXe: a new aerosol submodel for global simulations (v1), Geoscientific Model Development, 3, 391–412, doi:10.5194/gmd-3-391-2010, URL http://www.geosci-model-dev.net/3/391/2010/, 2010.

Sander, R., Kerkweg, A., Jckel, P., and Lelieveld, J.: Technical note: The new comprehensive atmospheric chemistry module MECCA, Atmospheric Chemistry and Physics, 5, 445–450, doi:10.5194/acp-5-445-2005, URL http://www.atmos-chem-phys.net/5/445/2005/, 2005.

Seinfeld, J. H. and Pandis, S. N.: Atmospheric chemistry and physics : from air pollution to climate change, J. Wiley, Hoboken, N.J., 2006.

Tobo, Y., Zhang, D., Nakata, N., Yamada, M., Ogata, H., Hara, K., and Iwasaka, Y.: Hygroscopic mineral dust particles as influenced by chlorine chemistry in the marine atmosphere, Geophysical Research Letters, 36, doi:10.1029/2008GL036883, URL http://doi.wiley.com/10.1029/2008GL036883, 2009.

Tost, H., Jockel, P., Kerkweg, A., Sander, R., and Lelieveld, J.: Technical note: A new comprehensive SCAVenging submodel for global atmospheric chemistry modelling, Atmos. Chem. Phys., 6, 565–574, doi:10.5194/acp-6-565-2006, URL http://www.atmos-chem-phys.net/6/565/2006/, 2006.

Twohy, C. H., Kreidenweis, S. M., Eidhammer, T., Browell, E. V., Heymsfield, A. J., Bansemer, A. R., Anderson, B. E., Chen, G., Ismail, S., DeMott, P. J., and Van Den Heever, S. C.: Saharan dust particles nucleate droplets in eastern Atlantic clouds, Geophysical Research Letters, 36, doi:10.1029/2008GL035846, URL http://www.agu.org/pubs/crossref/2009/2008GL035846.shtml, 2009.

Table 1: Revised manuscript – Modifications for referee#2. Please also note the modifications in Table 1 in our reply to referee #1.

no.	P. no.	L. no.	Before	Correction
1	7494	13	Our results show the importance of chemical aging and deposition of the dust during transport.	Our results show the importance of chemical aging of dust, which increases particles size, dust deposition and scavenging efficiency during transport, overall reducing the life-time relative to non-aged dust particles.
2	7496	11	Since Cyprus lows are often associated with precipitation, the residence time of dust particles in the atmosphere can be relatively short (approximately one day)	Since Cyprus lows are often associated with precipitation, the residence time of dust particles in the atmosphere can be relatively short. In case of a barometric trough penetrating from the Red Sea into the EM, it can be as short as one day (Dayan et al., 1991)
3	7496	13	Dayan et al. (1991, 2008)	Dayan et al. (2008)
4	7496	24	Especially the interaction between dust and anthropogenic pollution from eastern and western Europe (Levin et al., 2005) in addition to intercontinental air pollution transports from North America and Asia (Lelieveld et al., 2002) deserves attention, being the focus of this study	Especially the interaction of atmospheric dust particles with air pollution from eastern and western Europe and long-range transport from North America and Asia (Lelieveld et al., 2002; Levin et al., 2005, among others) remains to be scrutinized – the focus of this study.

Table 2: Continued.

no.	P. no.	L. no.	Before	Correction
5	7497	19	..., which can include a large fraction of water.	..., which can include a large fraction of water in case dust particles are coated by hydrochloric or nitric acids and/or are exposed to high relative humidity.
6	7499	11	After: ... (Fountoukis and Nenes, 2007).	Our model version distinguishes aerosol particles in 7 modes, 4 Soluble (nucleation, aitken, accumulation, coarse) and three INSoluble modes (aitken, accumulation, coarse) with the complexity of the aerosol thermodynamics as investigated in Metzger et al. (2006), by considering case F4 since ISORROPIA-II used here does not include organic salt compounds in the gas/aerosol partitioning and aerosol neutralization framework. Within EMAC, the dust particles are emitted online following Astitha et al. (2012) (e.g., governed by model dynamics, precipitation and soil moisture) in either the INSoluble accumulation and/or coarse mode and only upon aging and transport they can be transferred to the respective Soluble accumulation and/or coarse modes. The aging depends on the available condensable compounds calculated within the chemistry scheme (Sander et al., 2005). In addition, via coagulation and hygroscopic growth the size-distribution can change and small particles are transferred to larger sizes, i.e., for dust from accumulation to coarse, whereby hygroscopic growth of bulk dust and dust salt compounds is only allowed in the soluble modes.
7	7500	14	... and sulfate (SO_4^{2-})	... and sulfate (SO_4^{2-}) as tracers for the online calculated sea salt emissions.
8	7500	14	Added text before "This chemical speciation ..."	Additionally, K^+ is used for biomass burning emissions being emitted here only in the insoluble aitken mode.

Table 3: Continued.

no.	P. no.	L. no.	Before	Correction
9	7500	19	Added text	The dust particles can be present in our set-up in four modes, each represented by various calcium compounds that chemically characterize the bulk dust emissions depending on the level of aging. We account for the water uptake of various major mineral salt compounds, i.e., $CaSO_4$, $Ca(NO_3)_2$, $CaCl_2$, $MgSO_4$, $Mg(NO_3)_2$, $MgCl_2$, Na_2SO_4, $NaNO_3$, $NaCl$, K_2SO_4, KNO_3, KCl. Thus, We have limited the dust neutralization reactions in this work to calcium to be able to separate the dust associated water uptake and associated aging from sea salt effects. Since our set-up is flexible, the level of aerosol neutralization complexity can/will be changed for other application tasks. Within GMXe, the aging of dust aerosols depends on the total particle surface area and on the concentrations of the aerosol precursor gases (Pringle et al., 2010). The uptake of gases is kinetically limited considering random motion and diffusion processes that govern the condensation. The rate constant for the condensation on dust particles is given by Eq. 1 $$D_{flux} = \frac{4\pi D_f^2 r_w}{\frac{4D_f}{\nu r_w a_i} + \frac{r_w}{r_w + z_{f1}}} \quad (1)$$ where r_w is the ambient (wet) radius, D_f the temperature dependent diffusion coefficient defined by $D_f = 0.073\ P \left(\frac{T}{T_{ref}}\right)^{\frac{3}{2}}$, P the pressure, T the temperature and T_{ref} the reference temperature (298.15 K), ν denotes the particle mean velocity, defined by $\sqrt{\frac{8R_gT}{\pi M_g}}$, with R the gas constant (8.31 $Jmol^{-1}K^{-1}$), M_g the molar mass, z_{f1} the mean free path length of the kinetic regime, and a_i the accommodation coefficient (Fuchs and Davies, 1989; Seinfeld and Pandis, 2006). In the current setup we use the accommodation coefficients 0.1, 0.01, 0.01 for sulfuric, hydrochloric and nitric acid, respectively. These values have been empirically determined by a comprehensive modeling analysis, which will be presented separately. The uptake of acids is calculated for each particles size, i.e., for dust for the insoluble accumulation and coarse mode. For the current modeling study though, this set-up represents the dust air-pollution dynamics over the Eastern Mediterranean well.

Table 4: Continued.

no.	P. no.	L. no.	Before	Correction
10	7506	19	... at this elevation.	... at this elevation and the dust loading is significantly reduced as the frontal system passed through.
11	7508	13-16	For this case, both the model and the CALIPSO results show that dust was removed during transport from the atmosphere by wet and dry deposition, since the height of 15 the dust plume decreases from about 4000 m over the central Mediterranean on 21 September to about 2000 m over the EM on 22 September.	For both cases, the model and CALISPO results show that the dust concentration decreased during the transport and the height of the dust plume decreased from about 4000m over the central Mediterranean on 21 September to about 2000m over the EM on 22 September. The model results showed that the dust loading has significantly reduced after the frontal system has passed (Fig. 8) which enhanced the dust deposition (see next section).
12	7508	16	This is also confirmed by the independent LIDAR ground observations at CUT-TEPAK station (Mamouri et al., 2013)	removed.
13	7513	25	dust is rapidly aged	dust is aged.
14	7516	1	Added reference	Fuchs, N. A. and Davies, C. N.: The mechanics of aerosols, Dover Publications, New York, 1989.
15	7516	24	Added reference	Kanitz, T., Ansmann, A., Foth, A., Seifert, P., Wandinger, U., Engelmann, R., Baars, H., Althausen, D., Casiccia, C., and Zamorano, F.: Surface matters: limitations of CALIPSO V3 aerosol typing in coastal regions, Atmospheric Measurement Techniques, 7, 20612072, doi:10.5194/amt-7-2061-2014, http://www.atmos-meas-tech.net/7/2061/2014/, 2014.

Table 5: Continued.

no.	P. no.	L. no.	Before	Correction
16	7517	17	Added reference	Mamouri, R. E. and Ansmann, A.: Estimated desert-dust ice nuclei profiles from polarization lidar: methodology and case studies, Atmospheric Chemistry and Physics, 15, 34633477, doi:10.5194/acp-15-3463-2015, http://www.atmos-chem-phys.net/15/3463/2015/, 2015.
17	7517	17	Added reference	Mamouri, R. E. and Ansmann, A.: Fine and coarse dust separation with polarization lidar, At- mospheric Measurement Techniques, 7, 37173735, doi:10.5194/amt-7-3717-2014, http://www. atmos-meas-tech.net/7/3717/2014/, 2014.
18	7518	5	Added reference	Nisantzi, A., Mamouri, R. E., Ansmann, A., and Hadjimitsis, D.: Injection of mineral dust into the free troposphere during fire events observed with polarization lidar at Limassol, Cyprus, At- mospheric Chemistry and Physics, 14, 1215512165, doi:10.5194/acp-14-12155-2014, http: //www.atmos-chem-phys.net/14/12155/2014/, 2014.
19	7519	12	Added reference	Seinfeld, J. H. and Pandis, S. N.: Atmospheric chemistry and physics : from air pollution to climate change, J. Wiley, Hoboken, N.J., 2006.

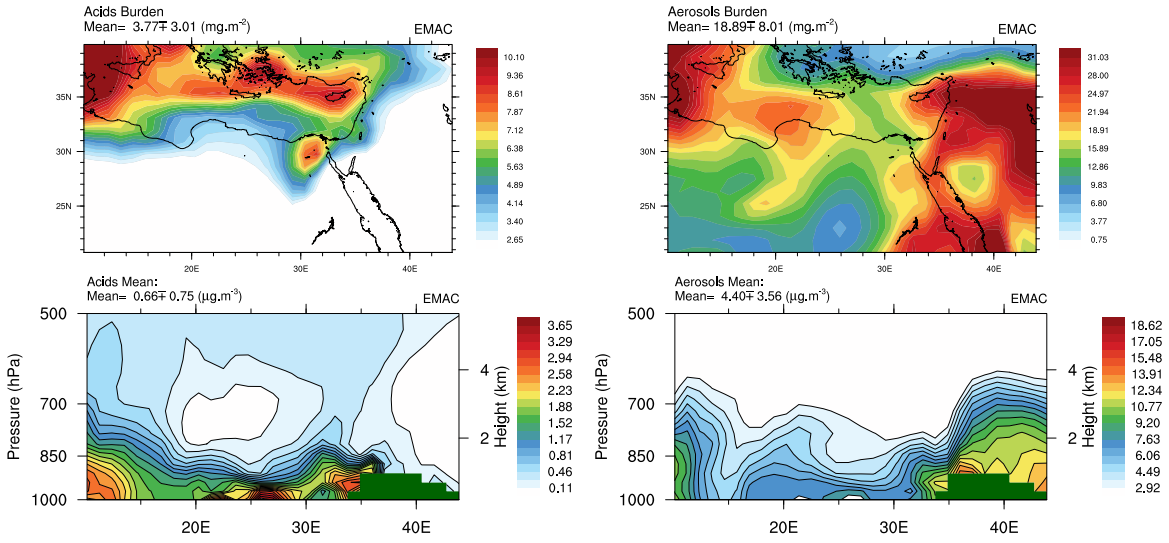

Figure 1: Air pollution loadings over the EM (average 20^{th} September - 1^{st} October 2011). The air pollution loading represents the vertical integral (burden) of the mass concentration $[mg\ m^2]$ of (left) total inorganic acids ($HCl+HNO_3+H_2SO_4$) that are present in the gas phase, maintaining gas-aerosol equilibrium, (right) the corresponding lumped aerosol burden ($SO_4^{2-}+HSO_4^-+NO_3^-+NH_4^+ +H_2SO_4$); both average over 20^{th} September - 1^{st} October 2011. This figure is added to the supplement.